ELSEVIER

Journal of Organometallic Chemistry 630 (2001) 221–243

Journal of Organometallic Chemistry

www.elsevier.com/locate/jorganchem

Chiral chelate phosphanes☆ XI. Application of cyclopentane-based C_2 chiral bis(phosphane) ligands $C_5H_8(PR_2)_2$ to Pt–Sn-catalyzed styrene hydroformylation

Lutz Dahlenburg *, Stefan Mertel

Institut für Anorganische Chemie der Friedrich-Alexander-Universität Erlangen-Nürnberg, Egerlandstrasse 1, D-91058 Erlangen, Germany

Received 7 March 2001; accepted 14 March 2001

Dedicated to Professor Dr Dieter Sellmann on the occasion of his 60th birthday.

Abstract

Treatment of [(1,5-C_8H_{12})PtCl(X)] (X = Cl, CH_3, CH_2CMe_3) with C_2 chiral cyclopentane-1,2-diyl-bis(phosphanes) $C_5H_8(PR_2)_2$, either as racemic mixtures or as resolved enantiomers, afforded the chelate complexes [$C_5H_8(PR_2)_2Pt(Cl)(X)$] (X = Cl: R = Ph (**1**), *N*-pip (**2**), OPh (**3**); X = CH_3: R = Ph (**4**), *N*-pip (**5**), OPh (**6**); X = CH_2CMe_3: R = Ph (**7**), *N*-pip (**8**), OPh (**9**); '*N*-pip' = $N(CH_2)_5$), (+)-[(1*R*,2*R*)-$C_5H_8\{P(OPh)_2\}_2PtCl_2$] [(***R*,*R*)-3**], (−)-[(1*S*,2*S*)-$C_5H_8\{P(OPh)_2\}_2PtCl_2$] [(***S*,*S*)-3**], (−)-[(1*R*,2*R*)-$C_5H_8(PPh_2)_2Pt(Cl)(X)$], and (+)-[(1*S*,2*S*)-$C_5H_8(PPh_2)_2Pt(Cl)(X)$] (X = CH_3: (***R*,*R*)-4**, (***S*,*S*)-4**; X = CH_2CMe_3: (***R*,*R*)-7**, (***S*,*S*)-7**). Reacting **4**, **6**, and **7** with AgO_3SCF_3 led to triflate derivatives [$C_5H_8(PR_2)_2Pt(X)(OSO_2CF_3)$] [X = CH_3: R = Ph (**11**), OPh (**12**); X = CH_2CMe_3: R = Ph (**13**)] with covalently bonded OSO_2CF_3 ligands. The unusual Pt_2 complex [μ-Cl$\{C_5H_8(PPh_2)_2PtCH_3\}_2$]$O_3SCF_3$ (**14**) containing an unsupported single Pt–Cl–Pt bridge was also isolated. In the presence of $SnCl_2$, complexes **1**, **3**, **4**, **6**, **7**, and **9** are catalysts for the hydroformylation of styrene forming 2- and 3-phenylpropanal together with ethylbenzene. Except for **1**, they also catalyze the consecutive hydrogenation of the primary propanals to alcohols. High regioselectivities towards 2-phenylpropanal (branched-to-normal ratios ≥ 91:9) were obtained in hydroformylations catalyzed by **3** and **4**, for which the influence of varied CO/H_2 partial pressures, catalyst-to-substrate ratios and different reaction temperatures and times on the outcome of the catalytic reaction was also studied. When tin-modified complexes (***R*,*R*)-3**, (***S*,*S*)-3**, and (***S*,*S*)-4** were used as optically active Pt(II) catalysts, an only low stereoselectivity for asymmetric hydroformylation (*e.e.* < 18%) was observed. The Pt–Sn complexes [$C_5H_8(PR_2)_2Pt(CH_3)(SnCl_3)$] [R = Ph (**15**), OPh (**17**)], resulting from $SnCl_2$ insertion into the Pt–Cl bonds of **4** or **6**, undergo rapid degradation in solution, forming mixtures composed of [$C_5H_8(PR_2)_2Pt(X)(Y)$] with R = Ph or OPh and X/Y = Cl/$SnCl_3$ (**16**, **18**), Cl/Cl (**1**, **3**), and $SnCl_3/SnCl_3$ (**19**, **20**), respectively. In the presence of $SnCl_2$, triflate complex **11** also becomes a catalyst for styrene hydroformylation and consecutive hydrogenation of the aldehydes to alcohols. The crystal structures of 11 complexes — **2**, **5**, **7**, **8**, **9**, **10** (the previously prepared [$C_5H_8\{P(N\text{-pip})_2\}_2Pt(CH_2CMe_3)_2$]), **13**, **14**, **16**, (***R*,*R*)-3**, and (***S*,*S*)-3** — were determined by X-ray diffraction. © 2001 Elsevier Science B.V. All rights reserved.

Keywords: Chirality; *P* ligands; Platinum; Catalysis; Hydroformylation; X-Ray structure analysis

1. Introduction

Asymmetric hydroformylation of prochiral olefins such as vinyl arenes is potentially a very powerful tool for the synthesis of enantiomerically pure aldehydes, provided that the chemo-, regio- and enantioselectivity all prove to be excellent [2]. In pioneering contributions by Pittman, Consiglio, and Stille [3,4] and, more recently, in a communication by Cserépi-Szücs and Bakos [5a], good to very high enantiomeric excesses of branched aldehydes could be attained with $SnCl_2$-activated [{bis(phosphane)}$PtCl_2$] and [{bis(phosphite)}-$PtCl_2$] catalyst systems. In contrast to the extremely successful Rh-based systems utilizing chiral bidentate bis(phosphites) or phosphane–phosphites as supporting

☆ Part X: [1].

* Corresponding author. Tel.: +49-9131-85-27353; fax: +49-9131-85-27387.

E-mail address: dahlenburg@chemie.uni-erlangen.de (L. Dahlenburg).

0022-328X/01/$ - see front matter
PII: S0022-328X(01)01001-4

ligands [2d,6,7,8,9,10], Pt–Sn catalysts exhibiting high enantioselectivities, however, frequently suffer from low or, at best, moderate regioselectivities and the formation of substantial amounts of undesired hydrogenation products [2b], [{(*R*,*R*)-bco-dpb}$PtCl_2$]–$SnCl_2$ [3c] being a noteworthy exception (bco-dpb is {bicyclo[2.2.2]-octane-3,4-diyl-bis(methylene)}bis(5*H*-benzo[*b*]phosphindole). Conversely, high regioselectivities towards branched aldehydes but low optical and chemical yields were obtained with platinum–tin catalytic systems supported by bis(phosphite) ligands containing binaphthyl [5b] and, respectively, carbohydrate [11] backbones.

A large part of our current research is focused on bidentate phosphorus ligands of the type $C_5H_8(PR_2)_2$ (R = *C*-, *N*-, or *O*-bonded group) bearing differently substituted and, hence, fine-tunable donor sets supported on a C_2 chiral 1,2-*trans*-disubstituted cyclopentane framework [12,13]. Use of such ligands in transition metal-mediated asymmetric catalysis can provide insight into the relations and regularities existing between the performance of the catalytic system and the stereoelectronic properties of the active metal–ligand template [13h,14]. One aspect of the work reported in this communication was to elucidate how the chemo- and regioselectivities of styrene hydroformylation reactions are affected by differently substituted catalysts of the type $[C_5H_8(PR_2)_2Pt(Cl)(X)]$–$SnCl_2$ with R = phenyl, $N(CH_2)_5$ ('*N*-pip'), or phenoxy, and X = Cl, CH_3, or CH_2CMe_3, respectively. Throughout these exploratory studies, the phosphorus ligands were employed as racemic mixtures. The capacity for enantioface discrimination was only investigated for selected optically active $[C_5H_8(PR_2)_2Pt(Cl)(X)]$–$SnCl_2$ catalysts featuring acceptable chemo- and regioselectivities. To the best of our knowledge, chiral bis(phosphonites) as represented by $C_5H_8[P(OR)_2]_2$, so far have not been utilized as supporting ligands for asymmetric olefin hydroformylation [15], in contrast to phosphites (vide supra) and phosphinites [16].

The role of the $SnCl_2$ or $SnCl_3^-$ additive in the Pt–Sn-catalyzed hydroformylation reaction [17–20] still remains somewhat ambiguous. Thus, catalytic systems have been developed [21–25] whose performance casts doubt upon the function of the trichlorostannate group as an indispensable Pt-bonded ligand, and ample evidence has been presented which strongly supports the interpretation of the primary role of the $SnCl_3^-$ ion as that of a good leaving group, favoring CO activation and Pt–acyl formation in cationic platinum complexes [17,20a,20b]. Sulfonic acid anions RSO_3^- (R = CH_3, CF_3, F) represent other examples of good leaving groups whose coordination behavior toward, e.g. Pt(II) is well known to vacillate between that of a moderate-to-good metal-bonded ligand and that of a cation-stabilizing non-bonded counter-ion [26–32]. It is therefore not surprising to see that alkene platinum(0) complexes [{bis(phosphane)}$Pt(\eta^2\text{-}C_2H_4)$] become active hydroformylation catalysts [25], if in situ promoted to either [{bis(phosphane)}$Pt(\eta^2\text{-}CH_2CH_2\text{–}H)]O_3SCF_3$ or [{bis(phosphane)}$Pt(X)OSO_2CH_3$] (X = H, C_2H_5) [28] by methanesulfonic acid. These observations and the interest in tin-free hydroformylation catalysts based on platinum [21–23,25] prompted us to also probe $[C_5H_8(PPh_2)_2Pt(CH_3)(OSO_2CF_3)]$ as an exemplary triflate-containing complex for its hydroformylation activity. Recently, a decrease in activity and enantioselectivity but an increase in regioselectivity towards the chiral branched aldehyde was observed for homogeneous [{bis(phosphane)}$PtCl_2$]–$SnCl_2$ catalysts modified by triflate additives [20d].

2. Results and discussion

2.1. Racemic chloro complexes and triflate derivatives: preparation and structures

The chelate complexes $[C_5H_8(PR_2)_2Pt(Cl)(X)]$ [X = Cl: R = Ph (**1**), *N*-pip (**2**), OPh (**3**); X = CH_3: R = Ph (**4**), *N*-pip (**5**), OPh (**6**); X = CH_2CMe_3: R = Ph (**7**), *N*-pip (**8**), OPh (**9**); see Scheme 1] were synthesized by reacting the corresponding P_2 ligand with the requisite 1,5-cyclooctadiene precursor [(1,5-C_8H_{12})Pt(Cl)(X)] (X = Cl [33a,33c], CH_3 [33b], CH_2CMe_3 [33d]) in 1:1 stoichiometry in dichloromethane at ambient conditions, similar to the procedures previously described for **8** and related dineopentyls such as, e.g. $[C_5H_8\{P(N\text{-}pip)_2\}_2Pt(CH_2CMe_3)_2]$ (**10**) [13d].

Satisfactory yields of the triflate derivatives $[C_5H_8(PR_2)_2Pt(X)(OSO_2CF_3)]$ [X = CH_3: R = Ph (**11**), OPh (**12**); X = CH_2CMe_3: R = Ph (**13**)] resulted from the addition, at room temperature, of compounds **4**, **6**, and **7** to solution-suspensions of equimolar quantities of AgO_3SCF_3 in dichloromethane. If the reactants were combined in the reversed order at low temperature, unchanged starting complex readily displaced the $CF_3SO_3^-$ ligand from the triflate product already formed, producing chloro-bridged $[\mu\text{-}Cl\{C_5H_8(PR_2)_2\text{-}PtX\}_2]O_3SCF_3$, as exemplified by $[\mu\text{-}Cl\{C_5H_8(PPh_2)_2\text{-}PtCH_3\}_2]O_3SCF_3$ (**14**), which was isolated on adding one equivalent of silver triflate in portions to a CH_2Cl_2 solution of $[C_5H_8(PPh_2)_2Pt(Cl)(CH_3)]$ (**4**) kept at −60 °C.

The $^{31}P\{^1H\}$-NMR spectra of the dichloro and (alkyl)chloro or (alkyl)sulfonato complexes displayed the expected ^{195}Pt-flanked A_2 and AB resonances requiring no further discussion. Due to the lack of a molecular mirror plane bisecting the R–P–R angles of the prochiral –PR_2 groups, the phenyl, piperidino, and phenoxy carbon atoms of the substituents become pairwise diastereotopic and are found to be sufficiently different

for their nonequivalence to be detected in the 75.5 MHz $^{13}C\{^1H\}$-NMR spectra. Except for the unique methylene carbon C-4 of the cyclopentane backbone, each of the ^{13}C nuclei of the ligands gives rise to a spin system of the AA′*X* or AB*X* limiting type, A/A′ and A/B representing the two (with respect to ^{13}C) magnetically non-equivalent ^{31}P nuclei of molecules $[C_5H_8(PR_2)_2$-$PtCl_2]$ or $[C_5H_8(PR_2)_2Pt(X)(Y)]$ [34,35]. In the complexes studied, these spin systems exhibit practically all the possible multiplicities that can arise for the associated *X* part sub-spectra, depending on the magnitude of the various P,C and P,P couplings between the nuclei involved [34] (see Section 4).

The molecular structures of eight of the compounds prepared as outlined before, including the previously described complexes **8** and **10** [13d], were determined by single-crystal X-ray diffraction and are shown in Figs. 1–8, selected bond lengths and valence and torsion angles being collected in the legends.

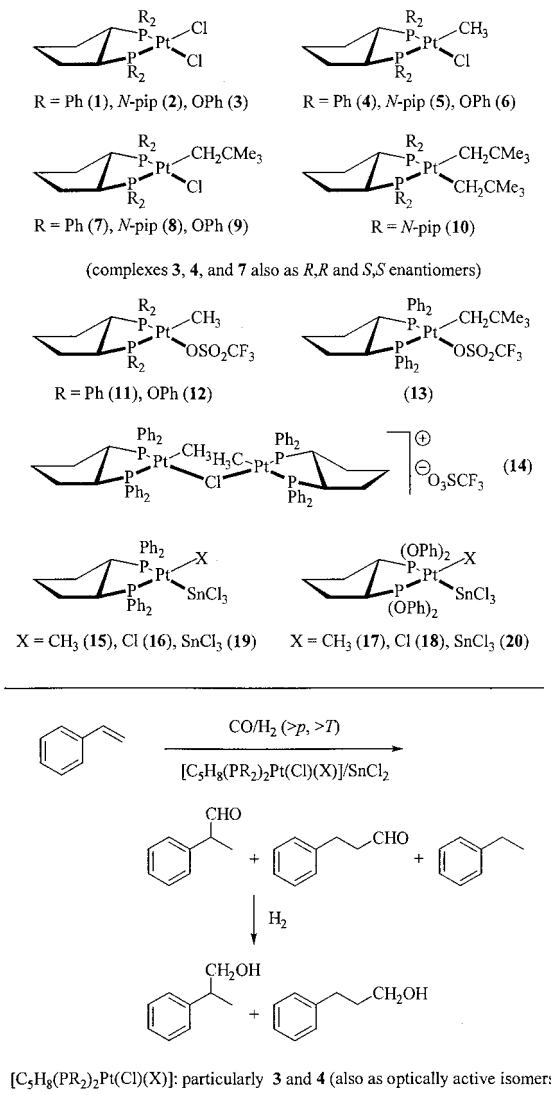

Scheme 1. Complexes and reactions studied.

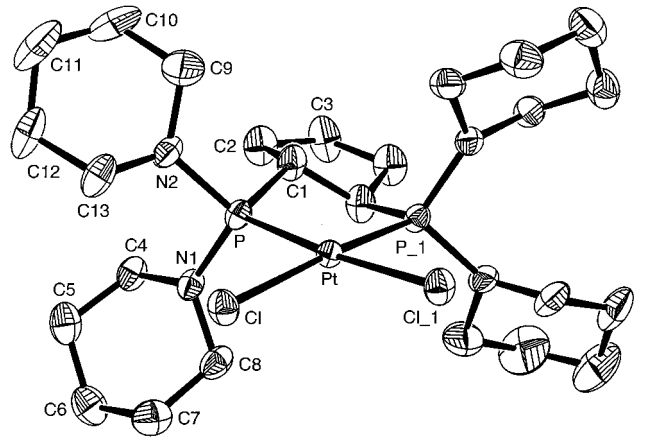

Fig. 1. Molecular structure of $[C_5H_8\{P(N\text{-pip})_2\}_2PtCl_2]$, **2**. Selected bond lengths (Å) and valence and torsion angles (°): Pt–Cl, 2.395(1); Pt–P, 2.226(1). Cl–Pt–Cl_1, 90.96(7); Cl–Pt–P, 90.81(5), Cl–Pt–P_1, 174.61(8); P–Pt–P_1, 87.90(8). P_1–Pt–P–N(1), 110.1(3); P_1–Pt–P–N(2), −127.6(3). Operators for generating equivalent atoms Cl_1 and P_1: $-x+\frac{1}{4}$, y, $-z+\frac{3}{4}$.

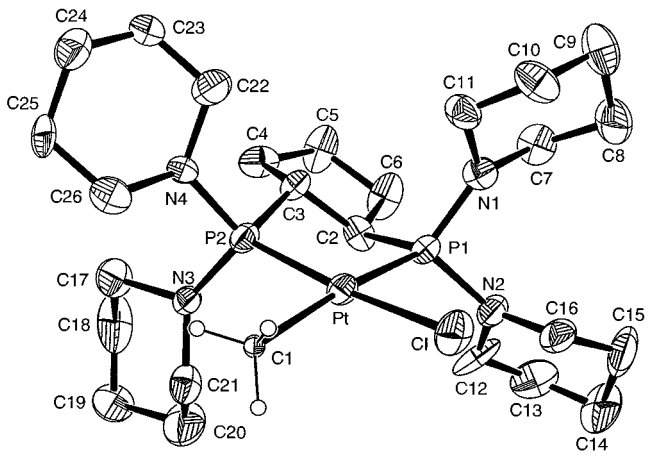

Fig. 2. Molecular structure of $[C_5H_8\{P(N\text{-pip})_2\}_2Pt(Cl)(CH_3)]$, **5**. Selected bond lengths (Å) and valence and torsion angles (°): Pt–Cl, 2.383(6); Pt–P(1), 2.276(6); Pt–P(2), 2.213(6); Pt–C(1), 2.206(16). Cl–Pt–P(1), 95.0(2); Cl–Pt–P(2), 171.4(2); Cl–Pt–C(1), 84.5(5); P(1)–Pt–P(2), 87.8(2); P(1)–Pt–C(1), 173.9(5); P(2)–Pt–C(1), 93.6(4). P(1)–Pt–P(2)–N(3), 108.6(8); P(1)–Pt–P(2)–N(4), −125.0(8); P(2)–Pt–P(1)–N(1), 105.2(8); P(2)–Pt–P(1)–N(2), −131.6(8).

The molecules show the expected planar coordination geometry about the central platinum atom as evidenced from: (i) the sum of the four intra- and interligand *cis* angles, found in the narrow range from 359.5 to 360.9°, and (ii) from the angles between the normals to the two planes defined by the PtP_2 and Pt(X)(Y) fragments. These dihedral angles lie between 2.9° (planes at Pt(1) in **14**) and 8.6° (complex **8**) and thus deviate only little from the ideal value of 0° required for an undistorted planar surrounding of the metal atom. As observed in earlier work for four related Pt(II) complexes bearing $C_5H_8(PR_2)_2$ ligands

[13d], the P–Pt–P bite-angles, ranging from 85.3 to 88.2°, show only a small degree of scattering.

The Pt–P bond lengths vary between 2.181 and 2.226 Å for chloride or triflate as weak *trans* influencing ligands and reveal no discernible dependence on the nature of the substituents on phosphorus. For some of the complexes studied, the lengths of the Pt–P bonds opposite the strongly *trans* bond-weakening methyl or neopentyl groups tend to be slightly shorter in molecules containing P–N- or P–O-substituted chelat-

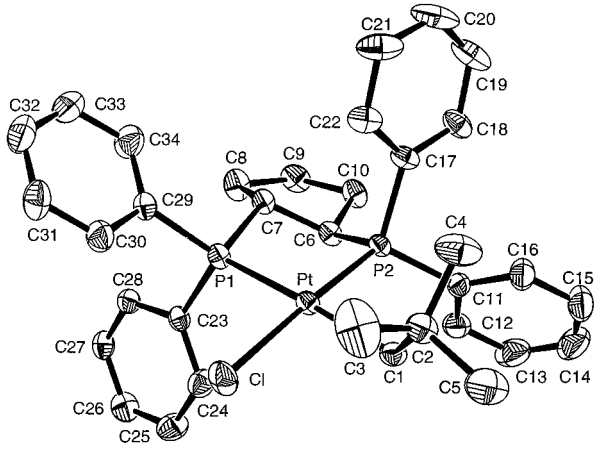

Fig. 3. Molecular structure of $[C_5H_8(PPh_2)_2Pt(Cl)(CH_2CMe_3)]$, **7**. Selected bond lengths (Å) and valence and torsion angles (°): Pt–Cl, 2.369(1); Pt–P(1), 2.344(1); Pt–P(2), 2.208(1); Pt–C(1), 2.101(5). Cl–Pt–P(1), 91.65(5); Cl–Pt–P(2), 173.52(7); Cl–Pt–C(1), 87.8(1); P(1)–Pt–P(2), 86.74(5); P(1)–Pt–C(1), 175.6(2); P(2)–Pt–C(1), 93.3(1). P(1)–Pt–P(2)–C(11), −140.0(2); P(1)–Pt–P(2)–C(17), 90.5(2); P(2)–Pt–P(1)–C(23), 110.6(2); P(2)–Pt–P(1)–C(29), −124.9(2).

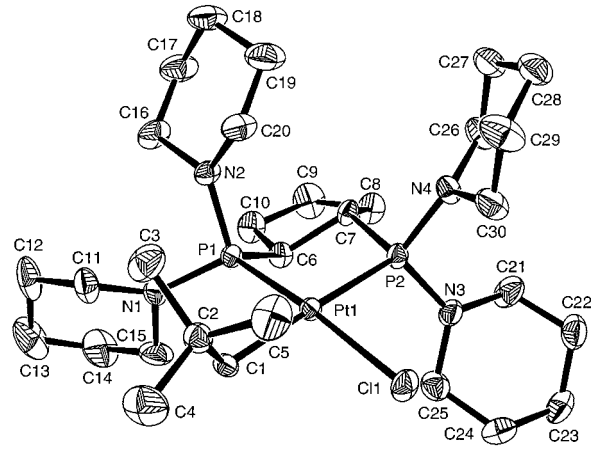

Fig. 4. Molecular structure of $[C_5H_8\{P(N\text{-pip})_2\}_2Pt(Cl)(CH_2CMe_3)]$, **8**. Selected bond lengths (Å) and valence and torsion angles (°): Pt(1)–Cl(1), 2.393(1); Pt(1)–P(1), 2.206(1); Pt(1)–P(2), 2.327(2); Pt(1)–C(1), 2.114(5). Cl(1)–Pt(1)–P(1), 171.38(6); Cl(1)–Pt(1)–P(2), 92.58(5); Cl(1)–Pt(1)–C(1), 86.5(1); P(1)–Pt(1)–P(2), 85.94(5); P(1)–Pt(1)–C(1), 94.7(1); P(2)–Pt(1)–C(1), 178.0(2). P(1)–Pt(1)–P(2)–N(3), −121.3(2); P(1)–Pt(1)–P(2)–N(4), 111.0(2); P(2)–Pt(1)–P(1)–N(1), 144.4(2); P(2)–Pt(1)–P(1)–N(2), −87.5(2).

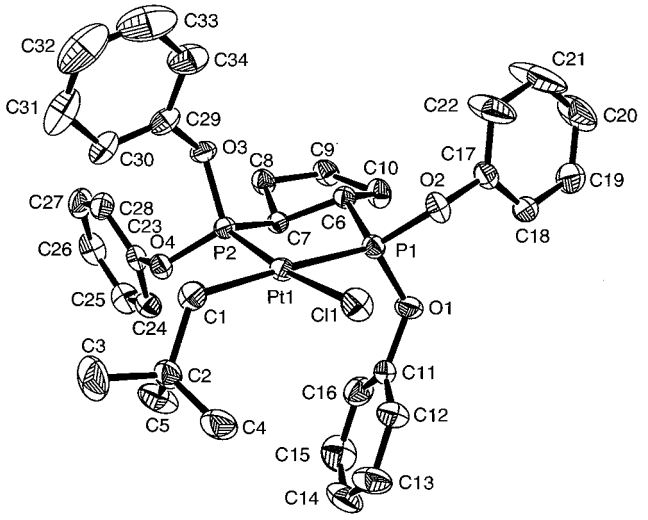

Fig. 5. Molecular structure of $[C_5H_8\{P(OPh)_2\}_2Pt(Cl)(CH_2CMe_3)]$, **9**. Selected bond lengths (Å) and valence and torsion angles (°): Pt(1)–Cl(1), 2.359(1); Pt(1)–P(1), 2.277(1); Pt(1)–P(2), 2.181(1); Pt(1)–C(1), 2.108(5). Cl(1)–Pt(1)–P(1), 90.99(5); Cl(1)–Pt(1)–P(2), 172.73(5); Cl(1)–Pt(1)–C(1), 88.8(2); P(1)–Pt(1)–P(2), 85.26(5); P(1)–Pt(1)–C(1), 177.9(2); P(2)–Pt(1)–C(1), 95.2(2). P(1)–Pt(1)–P(2)–O(3), −97.5(2); P(1)–Pt(1)–P(2)–O(4), 136.4(2); P(2)–Pt(1)–P(1)–O(1), −106.0(2); P(2)–Pt(1)–P(1)–O(2), 131.3(2).

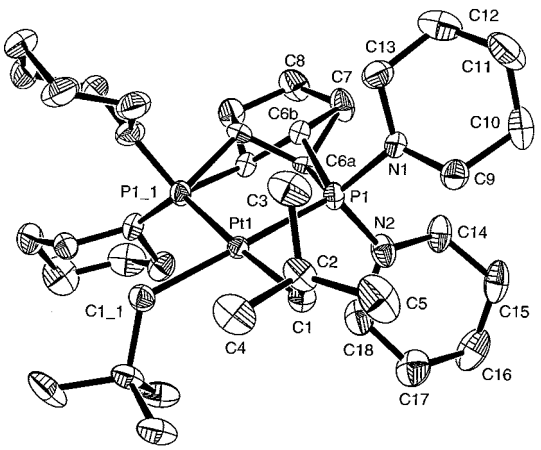

Fig. 6. Molecular structure of $[C_5H_8\{P(N\text{-pip})_2\}_2Pt(CH_2CMe_3)_2]$ (**10**) showing the twofold spatial disorder of ring atoms C(6a) and C(6b). Selected bond lengths (Å) and valence and torsion angles (°): Pt(1)–P(1), 2.285(1); Pt(1)–C(1), 2.135(5). P(1)–Pt(1)–P(1)_1, 86.38(7); P(1)–Pt(1)–C(1), 90.4(1); P(1)–Pt(1)–C(1)_1, 176.3(1); C(1)–Pt(1)–C(1)_1, 92.8(3). P(1)_1–Pt(1)–P(1)–N(1), 125.2(2); P(1)_1–Pt(1)–P(1)–N(2), −110.9(2). Operators for generating equivalent atoms P(1)_1 and C(1)_1: $-x, y, -z+\frac{1}{2}$.

ing ligands (**5**, **9**, **10**: *d*(Pt–P), 2.276(6)–2.285(1) Å; cf. 2.253(4)–2.307(3) Å for three similar compounds having $-P(NR_2)_2$ or $-P(OR)_2$ *trans* to neopentyl [13d]) than in those (**7**, **13**) derived from the P–C-bonded $C_5H_8(PPh_2)_2$ chelate system, where the corresponding Pt–P bonds are elongated to 2.344(1) and 2.346(2) Å, respectively. It is, however, questionable whether these differences mirror any meaningful influence of the indi-

vidual *P*-substituents on the bond lengths, since the Pt–P distances *trans* to the alkyl groups in $[C_5H_8\{P(N\text{-}pip)_2\}_2Pt(Cl)(CH_2CMe_3)]$ (**8**), 2.327(2) Å, and $[\mu\text{-}Cl\{C_5H_8(PPh_2)_2PtCH_3\}_2]O_3SCF_3$ (**14**), 2.312(3) and 2.325(2) Å, do not differ significantly. The non-bridging Pt–Cl distances fall within the narrow range 2.383(1)–2.395(1) Å for the complexes derived from the $C_5H_8[P(N\text{-}pip)_2]_2$ ligand (**2**, **5**, **8**), but are 2.359(1) Å for the *P*-phenoxy-substituted molecule **9** and 2.346(2) and 2.366(2) Å for two similar complexes having $C_5H_8[P(OR)_2]_2$ ligands [13d]. However, as with the Pt–P bond lengths discussed before, these variations should not be overestimated as the length of the Pt–Cl bond *trans* to PPh_2 in $[C_5H_8(PPh_2)_2Pt(Cl)(CH_2CMe_3)]$ (**7**), 2.369(1) Å, is very close to those of the molecules having $P(OR)_2$ donor sets opposite Pt–Cl. The Pt–C distances, 2.093(8)–2.206(16) Å, measured for the two methyl (**5**, **14**) and the five neopentyl (**7**–**10**, **13**) derivatives fall within the range from 2.02 to 2.22 Å typically spanned by Pt–sp^3-C bonds in organo complexes adopting approximately square-planar coordination geometry at platinum [36], the longer distances occurring when the alkyl group is facing a relatively strong *trans* influence ligand, such as a *P* donor. The Pt–OSO_2CF_3 distance in **13**, 2.173(5) Å, is significantly longer than that of 2.090(6) Å earlier reported for $[\{(C_2F_5)_2P(CH_2)_2P(C_2F_5)_2\}Pt(CH_3)(OSO_2CF_3)]$, featuring an unusually strong interaction between the triflate ligand and the electrophilic metal center [31], but compares well to the value of 2.181(9) Å measured for $[\{Bu^t_2P(CH_2)_3PBu^t_2\}Pt(H)(OSO_2CF_3)]$ [28b].

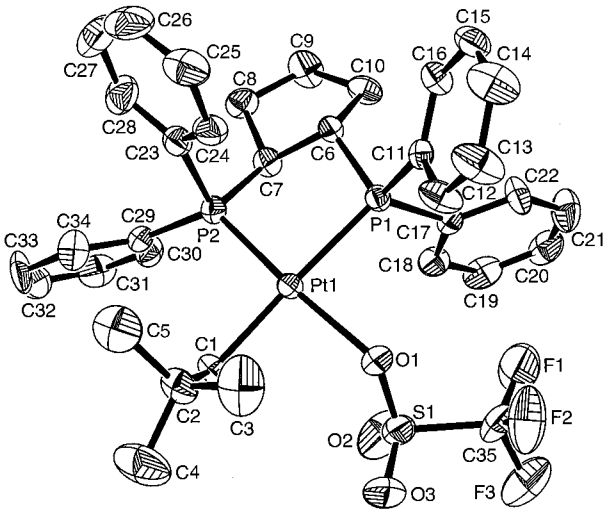

Fig. 7. Molecular structure of $[C_5H_8(PPh_2)_2Pt(CH_2CMe_3)(OSO_2CF_3)]$, **13**. Selected bond lengths (Å) and valence and torsion angles (°): Pt(1)–P(1), 2.346(2); Pt(1)–P(2), 2.189(2); Pt(1)–O(1), 2.173(5); Pt(1)–C(1), 2.105(7); S(1)–O(1), 1.458(6); S(1)–O(2), 1.403(7); S(1)–O(3), 1.422(7); S(1)–C(35), 1.81(1); C(35)–F(1), 1.29(1); C(35)–F(2), 1.30(1); C(35)–F(3), 1.33(1). P(1)–Pt(1)–P(2), 86.28(8); P(1)–Pt(1)–O(1), 89.2(1); P(1)–Pt(1)–C(1), 178.1(2); P(2)–Pt(1)–O(1), 174.4(2); P(2)–Pt(1)–C(1), 95.6(2); O(1)–Pt(1)–C(1), 89.0(3); Pt(1)–O(1)–S(1), 131.0(3); O(1)–S(1)–O(2), 114.7(4); O(1)–S(1)–O(3), 112.5(4); O(2)–S(1)–O(3), 117.6(5); O(1)–S(1)–C(35), 101.5(4); O(2)–S(1)–C(35), 104.4(5); O(3)–S(1)–C(35), 103.6(5); S(1)–C(35)–F(1), 112.9(7); S(1)–C(35)–F(2), 111.7(7); S(1)–C(35)–F(3), 110.4(8); F(1)–C(35)–F(2), 108.4(10); F(1)–C(35)–F(3), 108.0(9); F(2)–C(35)–F(3), 105.1(8). P(1)–Pt(1)–P(2)–C(23), −83.1(3); P(1)–Pt(1)–P(2)–C(29), 147.2(3); P(2)–Pt(1)–P(1)–C(11), 110.4(3); P(2)–Pt(1)–P(1)–C(17), −123.3(3).

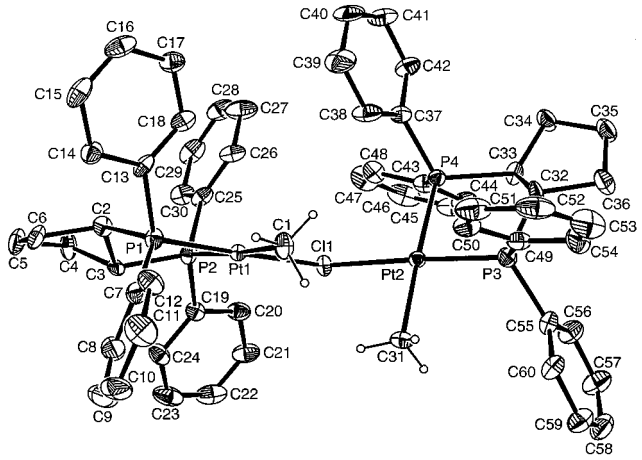

Fig. 8. Molecular structure of the binuclear cation of $[\mu\text{-}Cl\{C_5H_8(PPh_2)_2PtCH_3\}_2]O_3SCF_3$ (**14**); *meso* form shown; spatially disordered positions (2a), (2b), (32a), and (32b) of carbon atoms C(2), C(3), C(32), and C(33) omitted for clarity. Selected bond lengths (Å) and valence and torsion angles (°): Pt(1)–Cl(1), 2.405(2); Pt(1)–P(1), 2.192(3); Pt(1)–P(2), 2.325(2); Pt(1)–C(1), 2.093(8); Pt(2)–Cl(1), 2.399(2); Pt(2)–P(3), 2.190(3); Pt(2)–P(4), 2.312(3); Pt(2)–C(31), 2.113(9). Pt(1)–Cl(1)–Pt(2), 120.2(1); Cl(1)–Pt(1)–P(1), 177.97(8); Cl(1)–Pt(1)–P(2), 89.85(9); Cl(1)–Pt(1)–C(1), 92.5(3); P(1)–Pt(1)–P(2), 88.25(10); P(1)–Pt(1)–C(1), 89.4(3); P(2)–Pt(1)–C(1), 176.3(3); Cl(1)–Pt(2)–P(3), 176.96(10); Cl(1)–Pt(2)–P(4), 93.04(8); Cl(1)–Pt(2)–C(31), 88.1(3); P(3)–Pt(2)–P(4), 87.99(9); P(3)–Pt(2)–C(31), 90.7(3); P(4)–Pt(2)–C(31), 176.9(3). P(2)–Pt(1)–Cl(1)–Pt(2), 172.2(1); C(1)–Pt(1)–Cl(1)–Pt(2), −4.9(3); P(4)–Pt(2)–Cl(1)–Pt(1), −111.2(1); C(31)–Pt(2)–Cl(1)–Pt(1), 71.7(3); P(1)–Pt(1)–P(2)–C(19), −124.6(3); P(1)–Pt(1)–P(2)–C(25), 111.0(2); P(2)–Pt(1)–P(1)–C(7), 125.4(3); P(2)–Pt(1)–P(1)–C(13), −111.2(2); P(3)–Pt(2)–P(4)–C(37), −112.4(2); P(3)–Pt(2)–P(4)–C(43), 124.0(3); P(4)–Pt(2)–P(3)–C(49), 109.7(2); P(4)–Pt(2)–P(3)–C(55), −126.5(3).

In the strictly C_2 symmetric molecules $[C_5H_8\{P(N\text{-}pip)_2\}_2PtCl_2]$ (**2**) and $C_5H_8\{P(N\text{-}pip)_2\}_2Pt(CH_2CMe_3)_2]$ (**10**), the P–Pt–P–N torsion angles are close to 110° for an 'equatorial' alignment of the piperidino groups with respect to the coordination plane and become (with opposite sign) 125–127° for an 'axial' disposition, thereby indicating little axial-equatorial differentiation for the spatial orientation of these *P*-substituents. For the complexes having unlike anionic ligands attached to platinum, a similar situation is encountered for the PR_2 groups *cis* to chloride or methyl, where the P–Pt–P–R torsion angles amount to 105–112° and 124–132°, respectively. In the neopentyl derivatives **7**–**9** and **13**, on the other hand, the spatial arrangements of residues R in the PR_2 groups *cis* to the very bulky CH_2CMe_3

ligand differ significantly, the P–Pt–P–R torsion angles varying from 83 to 97° for the axial disposition and (again with opposite sign) from 136 to 147° for the equatorial orientation.

The bridging of two non-bonded platinum centers by a *single* μ-X ligand to form discrete binuclear molecules, as observed for **14**, has little precedence, except for a few $[\mu\text{-H}\{(R_3P)_2PtX\}_2]^+$ cations (R = Me, Et; X = H, Ph, C_6F_5) similarly containing unsupported Pt–H–Pt bridges [37] and some 'A-frame'-like compounds featuring additional bridging by bis(phosphanes) of the $R_2PCH_2PR_2$ type, such as $[Pt_2\{C(O)Me\}_2(\mu\text{-Cl})(\mu\text{-dppm})_2]Cl$ [38]. In binuclear cation **14**$^+$, the coordination planes of the two metals, which are 4.1633(5) Å apart, are twisted about the bridging chloro ligand such that the angle between the normals to the best l.s.q. planes spanned by the platinum and the four donor atoms is 65.6°. Associated torsion angles also defining this 'skewed' conformation are 71.7° for the C(31)–Pt(2)–Cl(1)–Pt(1) chain and −111.2° for the P(4)–Pt(2)–Cl(1)–Pt(1) chain (Fig. 8). In structurally characterized $[\mu\text{-H}\{(R_3P)_2PtX\}_2]^+$ complexes, the Pt···Pt distances are close to 3.0 Å, the two coordination planes being nearly perpendicular to each other [37]. The sharply distinct *trans* influences of the methyl and μ-Cl ligands are evident from the shrinkage of the Pt–P bonds facing the bridge (average 2.191 Å) as opposed to the stretching of the Pt–P linkages opposite CH_3 (mean 2.319 Å). Two nearly identical Pt–Cl distances, 2.399(2) and 2.405(2) Å, point to an essentially symmetric Pt–Cl–Pt linkage, similar to the situation encountered for the more common double-bridged $Pt_2(\mu\text{-X})_2$ systems, e.g. $[Pt_2(\mu\text{-Cl})_2\{Bu^t_2P(CH_2)_3PBu^t_2\}_2]BF_4$, where d(Pt–Cl) = 2.4007(6) and 2.4051(7) Å [39]. While the angle at the bridging chloro ligand of the latter complex is 102.67(1)°, the Pt–Cl–Pt angle in the unsupported single bridge of **14**$^+$ is increased to 120.2(1)°.

2.2. Racemic $[C_5H_8(PR_2)_2Pt(Cl)(X)]$–$SnCl_2$ catalysts (X = Cl, alkyl): styrene hydroformylation under different reaction conditions and related chemistry

The preformed dichloro and alkyl(chloro) complexes $[C_5H_8(PPh_2)_2Pt(Cl)(X)]$ [X = Cl (**1**), CH_3 (**4**), CH_2CMe_3 (**7**)], $[C_5H_8\{P(N\text{-pip})_2\}_2Pt(Cl)(X)]$ [X = CH_3 (**5**), CH_2CMe_3 (**8**)], and $[C_5H_8\{P(OPh)_2\}_2Pt(Cl)(X)]$ [X = Cl (**3**), CH_3 (**6**), CH_2CMe_3 (**9**)] were inspected for their performance as catalysts of the Pt–Sn-promoted hydroformylation of styrene as model substrate. $[C_5H_8\{P(N\text{-pip})_2\}_2PtCl_2]$ (**2**) was excluded from these studies because of its limited solubility. In these probing reactions, which were run for 66 h at typical platinum-to-olefin ratios of 1:170–1:180, in the presence of two equivalents of added anhydrous $SnCl_2$, in toluene solutions heated at 80 °C under 80 bar of a 1:1 CO–H_2 synthesis gas mixture, the use of $SnCl_2$-modified *P*-piperidino-substituted complexes **5** and **8** as catalysts led to good aldehyde selectivities (80–90%) but resulted in low conversion and virtually no selectivity for the branched product (Table 1). It was decided, therefore, to exclude these systems from further investigation. Catalysts containing $C_5H_8(PPh_2)_2$ or $C_5H_8[P(OPh)_2]_2$ ligands (Table 1; catalysts **1**, **4**, **7**, and **3**, **6**, **9**, respectively) effected quantitative conversion of the substrate within the reaction time chosen. In general, chemoselectivities for the aldehydes, however, decreased substantially (to ~50% and below) on substituting these bis(phosphane) and bis(phosphonite) complexes for the $[C_5H_8\{P(N\text{-pip})_2\}_2Pt(Cl)(X)]$ catalyst precursors, except for $[C_5H_8(PPh_2)_2PtCl_2]$ (**1**), producing the two propanals in 73% chemical yield and forming ethylbenzene as the exclusive accompanying product. In contrast, use of alkyl(chloro) complexes **4** and **7** or of all three bis(phosphonite)-containing compounds **3**, **6**, and **9** as pre-catalysts not only resulted in competitive hydrogenation of the styrene substrate but also induced consecutive reduction of the initially produced isomeric

Table 1
$[C_5H_8(PR_2)_2Pt(Cl)(X)]$–$SnCl_2$-catalyzed styrene hydroformylation: behavior of different platinum catalysts

$[C_5H_8(PR_2)_2Pt(Cl)(X)]$ catalyst; R, X	Conversion (%)	Aldehydes (%)	*b*/*n* ratio	Ethylbenzene (%)	3-Phenylpropanol (%)
1; Ph, Cl	100	73	68:32	27	–
4; Ph, CH_3	100	47	94:6	32	21
7; Ph, CH_2CMe_3	100	50	91:9	32	18
5; *N*-pip, CH_3	53	89	57:43	11	–
8; *N*-pip, CH_2CMe_3	32	79	52:48	21	–
3; OPh, Cl	100	34	91:9	36	30
6; OPh, CH_3	100	53	65:35	35	12
9; OPh, CH_2CMe_3	100	50	75:25	~45	~5

0.012–0.013 mmol of Pt complex, 2 equiv. of $SnCl_2$, and 2.2 mmol of styrene in 3 ml of [D_8]toluene; T = 80 °C; $p(H_2) = p(CO)$ = 40 bar; t = 66 h. Entries in the tables represent the average values of, at least, duplicate runs. Percentages refer to the composition of the aldehyde–ethylbenzene–3-phenylpropanol product mixtures; 2-phenylpropanol was also identified but could not be quantified by ^{1}H-NMR because of its low concentration (≤5%).

Table 2
$[C_5H_8\{P(OPh)_2\}_2PtCl_2]$–$SnCl_2$-catalyzed styrene hydroformylation: influence of reaction time

Reaction time (h)	Conversion (%)	Aldehydes (%)	*b*/*n* ratio	Ethylbenzene (%)	3-Phenylpropanol (%)
66	100	34	91:9	36	30
40	100	43	89:11	39	28
20	100	44	88:12	33	23
13	100	68	66:34	29	3
10	91	69	45:55	31	–

0.013 mmol of Pt complex, 0.021 mmol of $SnCl_2$, and 2.2 mmol of styrene in 3 ml of $[D_8]$toluene; $T = 80$ °C; $p(H_2) = p(CO) = 40$ bar (see also legend to Table 1).

phenylpropanals to propanols (Scheme 1), complexes **6** and **9** being somewhat slower in this regard than **4** and **7** and, particularly, **3**; see Table 1. The low chemoselectivities to aldehydes achieved in these reactions therefore clearly originate from hydrogenation steps occurring subsequently to hydroformylation. The consecutive formation of alcohols from primary hydroformylation products has rarely been observed [20d,40] and was in fact unexpected, considering that $SnCl_2$-modified [{bis(phosphane)}Pt] catalysts, unlike many cobalt-containing catalysts [2c], in general, have little propensity to promote the production of alcohols from aldehydes. We are aware of only one further Pt–Sn catalytic system, $[\{(S,S)\text{-diop}\}Pt(C_2H_4)]$–$SnCl_2$ (diop = 2,2 - dimethyl - 4,5 - bis(diphenylphosphanylmethyl) - 1,3-dioxolane), where subsequent reduction of the isomeric phenylpropanals (total yield at 100% conversion, ~ 85%) to the corresponding alcohols (~ 3%) occurred in addition to competitive formation of ethylbenzene (~ 12%) [25a]. It should be noted, however, that successive hydrogenation of hydroformylation products appears to be quite common for platinum complexes activated by methanesulfonic acid or triflate additives (see under Section 2.4).

With regard to the six $[C_5H_8(PPh_2)_2Pt(Cl)(X)]$–$SnCl_2$ and $[C_5H_8\{P(OPh)_2\}_2Pt(Cl)(X)]$–$SnCl_2$ systems compiled in Table 1, good regioselectivities towards the branched product ($b/n \geq 9{:}1$) are seen for the two bis(-phosphane)-supported catalysts **4** and **7** as well as for dichloro complex **3** bearing a bis(phosphonite) ligand. Conversely, *b*/*n* ratios of only 3:1 and below were attained, if tin-modified dichloro derivative **1**, possessing the $C_5H_8(PPh_2)_2$ chelate, or alkyl(chloro) complexes **6** and **9** with $C_5H_8[P(OPh)_2]_2$ chelates were applied as hydroformylation catalysts. With two of the catalytic systems leading to enhanced regioselectivity at quantitative substrate conversion, $[C_5H_8\{P(OPh)_2\}_2PtCl_2]$–$SnCl_2$ and $[C_5H_8(PPh_2)_2Pt(Cl)(CH_3)]$–$SnCl_2$, styrene hydroformylation in toluene as routine solvent was also carried out at varied catalyst-to-substrate and CO/H_2 ratios as well as at different reaction temperatures and times.

Table 2 summarizes the yields of the various hydroformylation and hydrogenation products that were obtained if the reaction was carried out in the presence of $[C_5H_8\{P(OPh)_2\}_2PtCl_2]$–$SnCl_2$ for 10–66 h. The data show that at 80 °C under 80 bar of CO/H_2 (1:1), at a catalyst-to-substrate ratio of 1:170, aldehyde production predominates over >C=C< and –CH=O hydrogenation, if the reaction is stopped after 10–13 h. The competitive hydrogenation product ethylbenzene is formed in fairly constant portions of ca. $35 \pm 5\%$, irrespective of the reaction time. Consecutive reduction of the initially formed aldehydes to alcohols accounts for the observation that in experiments reaching 100% styrene conversion, the chemoselectivity to the hydroformylation products decreases with ongoing reaction time. The regioisomeric excess in 2-phenylpropanal is seen to increase from practically null at incomplete transformation of the olefin substrate to ~ 9:1 after complete consumption of the olefin. As the reaction progresses, this gain in regioselectivity roughly parallels the growing production of 3-phenylpropanol. It is therefore concluded that the high preferences for the branched aldehyde displayed by $[C_5H_8\{P(OPh)_2\}_2PtCl_2]$–$SnCl_2$ (and also by tin-modified complexes **4** and **7**; Table 1) in catalyses reaching quantitative transformation mirrors the successive hydrogenation reaction, where the unbranched aldehyde is reduced faster to 3-phenylpropanol than the branched product to 2-phenylpropanol. In fact, in all the product mixtures investigated, the latter (though identifiable by NMR) was present only at such low concentrations (< 5%) that could not be quantified accurately by spectroscopic means. Similar behavior was previously reported for $[\{(S,S)\text{-diop}\}Pt(C_2H_4)]$–$SnCl_2$ and, particularly, $[\{(S,S)\text{-diop}\}Pt(C_2H_4)]$–$CH_3SO_3H$, affording the propanol isomers with selectivities towards the linear alcohol ranging from 68 to 97% [25a].

Data relevant to the effect of temperature on the chemo- and regioselectivity of the $[C_5H_8(PPh_2)_2Pt(Cl)(CH_3)]$–$SnCl_2$-catalyzed reaction are collected in Table 3. Consistent with the results previously reported by others [41,42], hydroformylation is highly favored over competitive hydrogenation at low temperature (40 °C) but disfavored at high temperature (> 100 °C), where the reaction is accompanied by the formation of considerable amounts of unidentified side-

Table 3
$[C_5H_8(PPh_2)_2Pt(Cl)(CH_3)]$–$SnCl_2$-catalyzed styrene hydroformylation at 100% conversion: influence of temperature

T (°C)	Aldehydes (%)	b/n ratio	Ethylbenzene (%)	3-Phenylpropanol (%)
120 [a]	25	96:4	47	28
100	40	93:7	33	27
80	47	94:6	32	21
60	48	84:16	34	18
40	74	50:50	26	–

0.013 mmol of Pt complex, 0.025 mmol of $SnCl_2$, and 2.2 mmol of styrene in 3 ml of $[D_8]$toluene; $p(H_2) = p(CO) = 40$ bar; $t = 66$ h (see also legend to Table 1).

[a] Considerable quantities of other side-products, presumably oligomers, were formed as well.

products, probably resulting from styrene oligomerization [20d]. There also exists the frequently observed [2b] temperature range (60–100 °C) where the total aldehyde yield remains nearly unaffected. Consecutive reduction of the aldehydes to alcohols is not noticed at 40 °C but becomes more and more effective on raising the temperature. Again, faster hydrogenation of the unbranched aldehyde appears to contribute to the temperature dependence of the b/n regioselectivity, which is zero at 40 °C but increases sharply at higher temperatures. The rise in regioselection for 2-phenylpropanal which is seen on raising the reaction temperature is at variance with the opposite temperature dependence of the branched-to-normal selectivities found for several other [{bis(phosphane)}$PtCl_2$]–$SnCl_2$ catalytic systems, even though similar, albeit less distinct, behavior has been described for [{(*R*)-(+)-binap}$PtCl_2$]–$SnCl_2$ and [{(*S*,*S*)-diop}Pt(Cl)(CH_3)]–$SnCl_2$ catalysts [42b], where binap = 2,2′-bis(diphenylphosphanyl)-1,1′-binaphthyl.

The hydrogen and carbon monoxide partial pressures can also considerably influence the activity and selectivity of hydroformylation catalysts [2b]. With $[C_5H_8(PPh_2)_2Pt(Cl)(CH_3)]$–$SnCl_2$ as catalyst, both the chemo- and the regioselectivity are affected to a great extent by the CO and H_2 partial pressures, as demonstrated in Table 4 for a series of reactions performed with different (1:2–7:1) CO–H_2 mixtures at 80 bar total pressure. As frequently observed for Pt–Sn-based hydroformylation catalysts [2b,3a,41a,42,43], an increase in $p(CO)$ and decrease in $p(H_2)$ is found to suppress the unwanted competitive hydrogenation of the substrate, thereby enhancing the selectivity to aldehydes. This improvement in chemoselectivity, however, is accompanied by a drastic decline of the selectivity for the branched product, the b/n ratios falling from 96:4 and 94:6 for 1:2 and 1:1 CO/H_2 gas mixtures to 80:20 at the 3:1 CO/H_2 molar ratio and, eventually, to 66:34 for the 7:1 CO/H_2 synthesis gas. Such trend in regioselectivity differs from that reported for, e.g. [{(*R*)-(+)-binap}Pt(Cl)(X)]–$SnCl_2$ and [{(*S*)-(−)-MeO-biph}Pt(Cl)(X)]–$SnCl_2$ catalytic systems (MeO-biph = 2,2′-bis(diphenylphosphanyl)-6,6′-dimethoxy-1,1′-biphenyl; X = Cl, CH_3), for which the 2-/3-phenylpropanal isomeric ratio remains almost unchanged on varying the H_2 and CO partial pressures [42], but resembles the characteristics of the [{(*R*,*R*)-diop}$PtCl_2$]–$SnCl_2$ catalyst, likewise displaying lower b/n selectivities at higher CO/H_2 ratios [3a]. Successive aldehyde hydrogenation does not occur at high CO but low H_2 partial pressures ($CO/H_2 = 7{:}1$) and is also less important than competitive styrene hydrogenation, if the partial pressure of H_2 is raised to 53 bar, $p(CO)$ being simultaneously lowered to 27 bar. This makes it difficult to conclude about the contribution of the consecutive reaction to the dependence of the branched-to-normal selectivities on the composition of the syn-gas mixture. Qualitatively, however, the lowest b/n regioselectivity is once more seen under conditions where reduction of the aldehydes to alcohols does not take place.

For the $[C_5H_8\{P(OPh)_2\}_2PtCl_2]$–$SnCl_2$-catalyzed reaction, the results summarized in Table 5 show the effect of varied Pt complex-to-styrene molar ratios on the aldehyde production and the branched-to-normal selectivity as well as on the competitive and consecutive formation of hydrogenated products. While the percentage of ethylbenzene in the final product mixtures ($\sim 35 \pm 5\%$) reveals only little dependence on the platinum-to-substrate ratio, the relative concentration of 3-phenylpropanol decreases from $\geq 20\%$ at the relatively high catalyst-to-styrene molar ratio of 1:170 to practically zero for the system containing the Pt–Sn catalyst and the substrate in 1:1200 stoichiometry. Over the same range, the total aldehyde yield is seen to increase, the preference for the branched product ($b/$

Table 4
$[C_5H_8(PPh_2)_2Pt(Cl)(CH_3)]$–$SnCl_2$-catalyzed styrene hydroformylation at 100% conversion: influence of CO and H_2 partial pressures

$p(CO)$ (bar)	$p(H_2)$ (bar)	Aldehydes (%)	b/n ratio	Ethylbenzene (%)	3-Phenylpropanol (%)
27	53	17	96:4	65	18
40	40	47	94:6	32	21
60	20	61	80:20	23	16
70	10	88	66:34	12	–

0.013 mmol of Pt complex, 0.025 mmol of $SnCl_2$, and 2.2 mmol of styrene in 3 ml of $[D_8]$toluene; $T = 80$ °C; $t = 66$ h (see also legend to Table 1).

Table 5
$[C_5H_8\{P(OPh)_2\}_2PtCl_2]$–$SnCl_2$-catalyzed hydroformylation of styrene at varied catalyst-to-substrate ratios

[Pt]-to-styrene molar ratio	Conversion (%)	Aldehydes (%)	b/n ratio	Ethylbenzene (%)	3-Phenylpropanol (%)
1:170	100	44	88:12	33	23
1:400	100	55	83:17	31	14
1:1200	100	61	56:44	39	–

0.013 mmol of Pt complex, 0.025 mmol of $SnCl_2$, and required amount of styrene in 3 ml of $[D_8]$toluene; $T = 80$ °C; $p(H_2) = p(CO) = 40$ bar; $t = 20$ h (see also legend to Table 1).

$n \sim 9{:}1$ at high platinum concentration), on the other hand, being lost simultaneously ($b/n \sim 1{:}1$ at high styrene concentration). This corroborates the interpretation that, for the systems under study, a preponderance of the branched hydroformylation product in the final reaction mixtures hardly reflects any inherent regioselectivity of the particular catalytic system but rather mirrors the successive hydrogenation of the formyl regioisomers, consuming 3-phenylpropanal in preference to 2-phenylpropanal. Given that $SnCl_2$-modified bis(phosphane)-coordinated platinum complexes normally behave as sluggish catalysts for hydrogenation reactions immediately following the hydroformylation step, the unexpected consecutive formation of alcohols points to the formation of some unrecognized platinum species being catalytically active for the reduction of the formyl group [20d], which so far, however, could not be revealed.

With regard to the generally accepted major steps of catalytic cycles proposed for the Pt–Sn assisted hydroformylation process, the active species in the mechanism initiated by complexes as different as $[PtL_2Cl_2]$ [44], $[PtL_2(H)(X)]$ [18,19,45], $[PtL_2(R)(X)]$ [17,18d,19], or $[PtL_2\{C(O)R\}(X)]$ [18a,18b,18e] (L = phosphane; X = Cl, $SnCl_3$; R = alkyl, aryl) is thought to be $[Pt(CO)(L)(H)(SnCl_3)]$. Similarly, the Pt–$SnCl_3$-bonded complexes $[\{Ph_2P(CH_2)_nPPh_2\}Pt(H)(SnCl_3)]$, $[\{Ph_2P(CH_2)_nPPh_2\}Pt(C_2H_5)(SnCl_3)]$, and $[\{Ph_2P(CH_2)_nPPh_2\}Pt\{C(O)C_2H_5\}(SnCl_3)]$ ($n = 3, 4$) were proposed as common key-intermediates involved in the hydroformylation of ethylene catalyzed by either $[\{Ph_2P(CH_2)_nPPh_2\}PtCl_2]$–$SnCl_2$ or $[\{Ph_2P(CH_2)_nPPh_2\}Pt(C_2H_5)(SnCl_3)]$ [18f]. On the other hand, more recent studies of the $[\{(S,S)\text{-bdpp}\}Pt(Cl)(CH_3)]$–$SnCl_2$ catalytic system (bdpp = 2,4-bis(diphenylphosphanyl)pentane) have shown that the presence of intermediates containing Pt–$SnCl_3$ bonds is indispensable *only* for the early stages of the catalytic cycle and that both carbonylation and aldehyde formation occur in four-coordinate cations possessing $SnCl_3^-$ counter-ions [20a,20b]. Furthermore, there are clear indications that alkyl trichlorostannato complexes resulting from [{bis(phosphane)}Pt(Cl)(alkyl)] precursors and $SnCl_2$ in the first step can easily decompose to form [{bis(phosphane)}$PtCl_2$] together with unknown tin products [18f,20b], thus facilitating the initialization of additional reaction channels and catalytic loops.

In order to gain an insight into the products originating from selected $[C_5H_8(PR_2)_2Pt(Cl)(alkyl)]$ catalyst precursors upon combination with tin(II) chloride, complex **4**, $[C_5H_8(PPh_2)_2Pt(Cl)(CH_3)]$, was allowed to interact with $SnCl_2$ in 1:1 stoichiometry in acetone at room temperature. Though the starting material was smoothly consumed within 10 min, no pure trichlorostannato product $[C_5H_8(PPh_2)_2Pt(CH_3)(SnCl_3)]$ (**15**) was obtained, a roughly 5:2:3 mixture of **15**, $[C_5H_8(PPh_2)_2Pt(Cl)(SnCl_3)]$ (**16**), and $[C_5H_8(PPh_2)_2PtCl_2]$ (**1**) being formed instead. Analogous treatment of $[C_5H_8\{P(OPh)_2\}_2Pt(Cl)(CH_3)]$ (**6**) with $SnCl_2$ in acetone similarly caused the production of $[C_5H_8\{P(OPh)_2\}_2Pt(CH_3)(SnCl_3)]$ (**17**), $[C_5H_8\{P(OPh)_2\}_2Pt(Cl)(SnCl_3)]$ (**18**), and $[C_5H_8\{P(OPh)_2\}_2PtCl_2]$ (**3**) in comparable molar ratio. Only if the reactants were combined at low temperature (−20 °C), tin(II) chloride was observed to cleanly insert into **6**, giving **17** as the almost exclusive complex, which at room temperature, however, underwent ready degradation to afford **18** and **3** as accompanying products. When the reaction between equimolar amounts of $SnCl_2$ and either **4** or **6** was carried out in toluene at 80 °C for 16–72 h, i.e. apart from the absence of syn-gas pressure under conditions typically applied during hydroformylation, the product mixtures were dominated by dichloro and bis(trichlorostannato) complexes, $[C_5H_8(PPh_2)_2PtX_2]$ [X = Cl (**1**), $SnCl_3$ (**19**)] and $[C_5H_8\{P(OPh)_2\}_2PtX_2]$ [X = Cl (**3**), $SnCl_3$ (**20**)], the corresponding mono-trichlorostannates **15**/**16** and **17**/**18** representing only minor constituents of the resulting product mixtures. When these reactions were run under 80 bar of synthesis gas, ^{31}P- and ^1H-NMR spectra taken immediately after depressurization indicated the presence of $[C_5H_8(PR_2)_2PtCl_2]$ together with acetaldehyde [$\delta(CHO) = 9.18$ (q, $J = 2.9$ Hz)]. No binuclear $[\{\mu\text{-}C_5H_8(PR_2)_2\}\{Pt(H)(R_2P)_2C_5H_8\}_2]^{2+}$, analogous to the diop- or bddp-containing diplatinum cations $[(\mu\text{-}P\cap P)\{Pt(H)(P\cap P)\}_2]^{2+}$ that were previously observed in CO/H_2-pressurized solutions of $[\{(S,S)\text{-bdpp}\}Pt(CH_3)(SnCl_3)]$ [20b] or $Pt/2e^-\|[(diop)PtCl_2]\|Sn/Sn^{2+}$ electrocatalysts [24], was however detected.

From the reactions studied, it is possible to propose two alternate (and perhaps competing) pathways on which the methyl group is removed from the $[C_5H_8(PR_2)_2Pt(Cl)(CH_3)]$–$SnCl_2$ systems during catalysis: (i) hydrogenolytic elimination of CH_3CHO from a platinum acetyl intermediate, possibly (though not necessarily) $[C_5H_8(PR_2)_2Pt(CO)\{C(O)CH_3\}]SnCl_3$ as an analogue of the bdpp-coordinated $[\{(S,S)\text{-bdpp}\}Pt(CO)\{C(O)CH_3\}]SnCl_3$ previously characterized by in situ high-pressure NMR spectroscopy [20a,20b]; (ii) $SnCl_2$-assisted conversion of $[C_5H_8(PR_2)_2Pt(Cl)(CH_3)]$ into $[C_5H_8(PR_2)_2Pt(X)(Y)]$ (X, Y = Cl, $SnCl_3$). Although the details of the latter transformation are unclear, it must be completely different from that previously postulated by Kollár and colleagues for the formation of $[\{(S,S)\text{-bdpp}\}PtCl_2]$ from $[\{(S,S)\text{-bdpp}\}Pt\{CH(CH_3)CO_2Et\}(SnCl_3)]$, where β-elimination of $CH_2{=}CHCO_2Et$ initially generates $[\{(S,S)\text{-bdpp}\}Pt(H)(SnCl_3)]$ which then is believed to undergo reductive elimination of $HSnCl_3$, followed by reaction of the resulting platinum(0) carbenoid with $CHCl_3$ solvent molecules [20b]. In earlier work by Scrivanti et al. [18f], the rapid decomposition of $[\{Ph_2P(CH_2)_nPPh_2\}Pt(C_2H_5)(SnCl_3)]$ to $[\{Ph_2P(CH_2)_nPPh_2\}PtCl_2]$ ($n = 3, 4$) occurring in solution in the absence of added ethylene was similarly accounted for by reductive elimination of $HSnCl_3$ from $[\{Ph_2P(CH_2)_nPPh_2\}Pt(H)(SnCl_3)]$ to produce $[\{Ph_2P(CH_2)_nPPh_2\}Pt(0)]$ as a reactive intermediate, which in turn was suggested to yield the final dichloride along with an unknown tin-containing by-product by extraction of chlorine from Sn–Cl bonds. Since β-elimination with formation of a transient hydride species cannot be operative for the degradation of methylplatinum complexes, an alternative mechanism has to be considered for the rapid transformation of $[C_5H_8(PR_2)_2Pt(Cl)(CH_3)]$ to dichloro, chloro(trichlorostannato), and bis(trichlorostannato) products $[C_5H_8(PR_2)_2Pt(X)(Y)]$, which takes place for chloro(methyl) complexes **4** and **6** in the presence of added tin(II) chloride. A conceivable sequence of reaction steps could involve C–Sn reductive elimination from the initially formed insertion products $[C_5H_8(PR_2)_2Pt(CH_3)(SnCl_3)]$ (**15**, **17**). Analogous C–Si and C–Ge elimination from $[(Me_2PhP)_2Pt(CH_3)(EPh_3)]$ (E = Si, Ge) has been described recently [46]. The 14e fragments $[C_5H_8(PR_2)_2Pt(0)]$ so generated can be expected to readily interact with eliminated CH_3SnCl_3 molecules, forming $[C_5H_8(PR_2)_2PtCl_2]$ which, in turn, will produce $[C_5H_8(PR_2)_2Pt(Cl)(SnCl_3)]$ (**16**, **18**) and $[C_5H_8(PR_2)_2Pt(SnCl_3)_2]$ (**19**, **20**) by (possibly reversible) $SnCl_2$ insertion (Scheme 2). The fate of the tin-containing residue, formally CH_3SnCl, could not be clarified unequivocally. Traces of light grey precipitates that might be elemental tin were observed occasionally. On the other hand, singlets flanked by tin satellites [δ = 0.68, 0.73; $J(^{117,119}Sn,H) = 42$ Hz], indicative of the presence of CH_3Sn groups in solution [47], were seen in the ^{1}H-NMR spectra of samples resulting from thermal treatment of $[C_5H_8(PPh_2)_2Pt(Cl)(CH_3)]$ (**4**) with $SnCl_2$ in toluene.

The above observations with $[C_5H_8(PR_2)_2Pt(Cl)(CH_3)]$–$SnCl_2$ lend further credence to the view that the catalytic results collected in Tables 1–5 are, at best, loosely associated with intrinsic ligand and complex properties of the respective catalysts but rather express the involvement in the catalytic cycle of several unrevealed species being active competitively.

As there exists only a single Pt–$SnCl_3$ complex containing a chelating bis(phosphane) ligand for which crystallographic information is available from the literature, viz. $[\{(S,S)\text{-bdpp}\}Pt(I)(SnCl_3)]$ [20c], the crystal structure of one of the trichlorostannato derivatives described before, $[C_5H_8(PPh_2)_2Pt(Cl)(SnCl_3)]$ (**16**), was determined. The structure consists of two independent molecules in the asymmetric unit, one of which possesses a rotationally disordered $SnCl_3$ ligand (Fig. 9). The coordination around the central metal is close to square planar, the PtP_2 planes being rotated with respect to those defined by Pt, Sn, and Cl at angles of 1.9° in molecule 2 and 5.4° in molecule 1. The Pt–Sn bond length averaged over the two crystallographically independent molecules of structure **16**, 2.567 Å, is shorter than the Pt–Sn distances measured for $[\{(S,S)\text{-bdpp}\}Pt(I)(SnCl_3)]$ (2.614 Å) [20c] and related $[(R_3P)_2Pt(X)(SnCl_3)]$ complexes (R = Ph, Cy; X = H, Cl; Pt–Sn, 2.590–2.601 Å) [19,48,49], but absolutely matches the range down to 2.478 Å observed for covalent Pt–$SnCl_3$ interactions [50]. Because of the substantial *trans* influence of the $SnCl_3$ ligand, the Pt–P bonds opposite Pt–Sn should be significantly longer than those opposite the metal-to-halogen bond. Rather unexpectedly, such bond-lengthening is, however, not apparent for complex **16** (mean *d*(Pt–P), 2.282 Å *trans* to $SnCl_3$ and 2.280 Å *trans* to Cl), as opposed to $[\{(S,S)\text{-}$

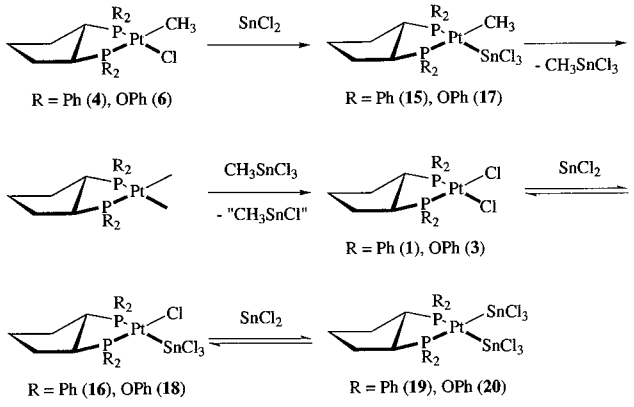

Scheme 2. Pathway proposed for the degradation of alkyl(trichlorostannato) complexes in solution.

bdpp}Pt(I)($SnCl_3$)], where the Pt–P distances amount to 2.300 Å with $SnCl_3^-$ as *trans*-bonded group but are shortened to 2.250 Å with iodide as *trans* ligand [20c]. We assume that the Pt–P bonds *trans* to Pt–Cl and, hence, *cis* to Pt–$SnCl_3$ in structure **16** are slightly elongated owing to steric repulsion between the PPh_2 and $SnCl_3$ groups in question. For molecule 1 (showing no $SnCl_3$ disorder), such hindrance is apparent from the Pt–Sn–Cl angles which increase from 117.5(2)° for Pt(1)–Sn(1)–Cl(2) to 120.2(2) and 123.1(2)° for Pt(1)–Sn(1)–Cl(3) and Pt(1)–Sn(1)–Cl(4), the joined Cl–Sn–Cl angles decreasing from 101.1(3)° for Cl(3)–Sn(1)–Cl(4) to 96.7(4)° and 93.3(3)° for Cl(2)–Sn(1)–Cl(3) and Cl(2)–Sn(1)–Cl(4), respectively. As observed for neopentyl complexes **7**–**9** and **13**, the P–Pt–P–C_{ipso} torsion angles (109–112° and, with opposite sign, 126–127°) indicate little axial–equatorial differentiation for the orientation of the phenyl substituents in the PPh_2 groups *cis* to chloride, whereas large differences in the axial–equatorial character are evident for the phenyl rings in the PPh_2 groups *cis* to the bulky $SnCl_3$ ligands: P–Pt–P–C_{ipso} torsion angles, 98–99° for the more axial and (with opposite sign) 135–136° for the more equatorial alignment.

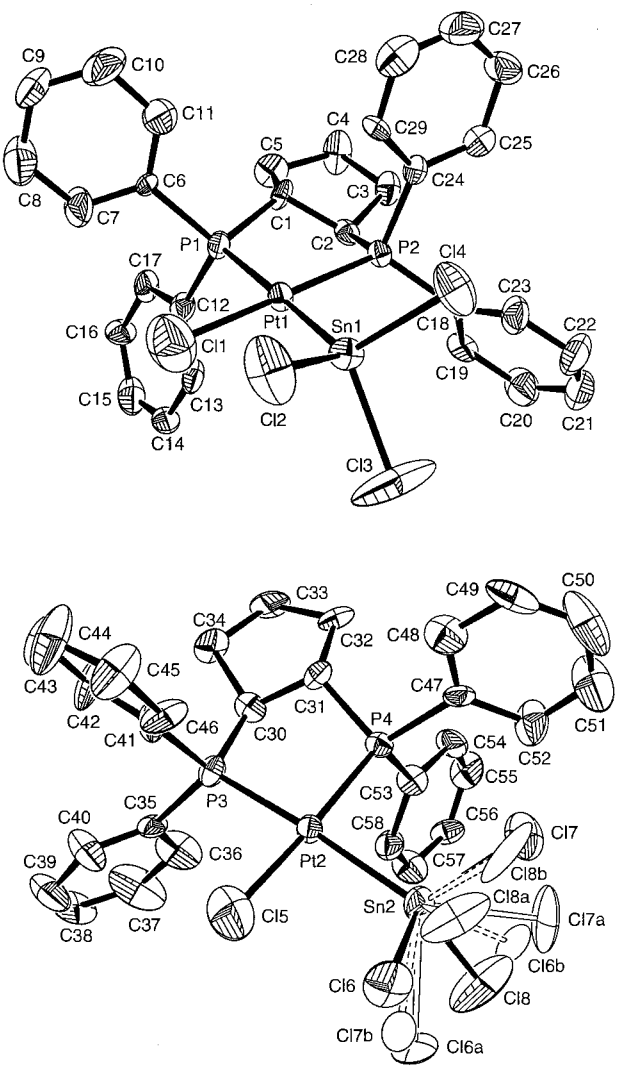

Fig. 9.

2.3. Styrene hydroformylation with optically active $[C_5H_8(PR_2)_2Pt(Cl)(X)]$ catalysts

Treatment of the substitutionally labile cyclooctadiene precursors [(1,5-C_8H_{12})Pt(Cl)(X)] (X = Cl, CH_3, CH_2CMe_3) with equimolar quantities of the $C_5H_8(PR_2)_2$ ligands as resolved (−)-(1*R*,2*R*)-/(+)-(1*S*,2*S*)-$C_5H_8[P(OPh)_2]_2$ and (+)-(1*R*,2*R*)-/(−)-(1*S*,2*S*)-$C_5H_8(PPh_2)_2$ enantiomers (see Section 4) allowed complexes **3**, **4**, and **7** to be prepared as optically active derivatives, viz. (+)-[(1*R*,2*R*)-$C_5H_8\{P(OPh)_2\}_2PtCl_2$] [(***R*,*R*)*-**3**], (−)-[(1*S*,2*S*)-$C_5H_8\{P(OPh)_2\}_2PtCl_2$] [(***S*,*S*)*-**3**], (−)-[(1*R*,2*R*)-$C_5H_8(PPh_2)$-Pt(Cl)(X)], and (+)-[(1*S*,2*S*)-$C_5H_8(PPh_2)$Pt(Cl)(X)], where X = CH_3 [(***R*,*R*)*-**4**, (***S*,*S*)*-**4**] and CH_2CMe_3 [(***R*,*R*)*-**7**, (***S*,*S*)*-**7**], respectively. Of these, the enantiomers (***R*,*R*)*-**3** and (***S*,*S*)*-**3** were isolated as monoclinic single crystals (space group $P2_1$) and fully characterized by X-ray analysis. A number of the bond lengths and angles given in the legends to Figs. 10 and 11 deviate

Fig. 9. Molecular structures of the two crystallographically independent molecules of [$C_5H_8(PPh_2)_2Pt(Cl)(SnCl_3)$] (**16**) showing the threefold rotational disorder of the $SnCl_3$ ligand in molecule 2. Selected bond lengths (Å) and valence and torsion angles (°) for molecule 1: Pt(1)–Sn(1), 2.572(2); Pt(1)–Cl(1), 2.283(9); Pt(1)–P(1), 2.281(5); Pt(1)–P(2), 2.275(5); Sn(1)–Cl(2), 2.363(7); Sn(1)–Cl(3), 2.326(8); Sn(1)–Cl(4), 2.359(6). Sn(1)–Pt(1)–Cl(1), 85.2(3); Sn(1)–Pt(1)–P(1), 173.5(1); Sn(1)–Pt(1)–P(2), 97.3(1); Cl(1)–Pt(1)–P(1), 90.6(3); Cl(1)–Pt(1)–P(2), 176.9(3); P(1)–Pt(1)–P(2), 87.0(2); Pt(1)–Sn(1)–Cl(2), 117.5(2); Pt(1)–Sn(1)–Cl(3), 120.2(2); Pt(1)–Sn(1)–Cl(4), 123.1(2); Cl(2)–Sn(1)–Cl(3), 96.7(4); Cl(2)–Sn(1)–Cl(4), 93.3(3); Cl(3)–Sn(1)–Cl(4), 100.1(3). P(1)–Pt(1)–P(2)–C(18), −136.0(8); P(1)–Pt(1)–P(2)–C(24), 99.5(8); P(2)–Pt(1)–P(1)–C(6), −126.7(8); P(2)–Pt(1)–P(1)–C(12), 109.6(7). — Selected bond lengths (Å) and valence and torsion angles (°) for molecule 2: Pt(2)–Sn(2), 2.562(2); Pt(2)–Cl(5), 2.289(9); Pt(2)–P(3), 2.283(6); Pt(2)–P(4), 2.286(5); Sn(2)–Cl(6), 2.40(2); Sn(2)–Cl(7), 2.35(3); Sn(2)–Cl(8), 2.36(2); Sn(2)–Cl(6a), 2.56(4); Sn(2)–Cl(7a), 2.43(4); Sn(2)–Cl(8a), 2.33(3); Sn(2)–Cl(6b), 2.45(3); Sn(2)–Cl(7b), 2.30(3); Sn(2)–Cl(8b), 2.27(4). Sn(2)–Pt(2)–Cl(5), 85.0(3); Sn(2)–Pt(2)–P(3), 175.8(1); Sn(2)–Pt(2)–P(4), 97.2(1); Cl(5)–Pt(2)–P(3), 90.9(3); Cl(5)–Pt(2)–P(4), 177.2(3); P(3)–Pt(2)–P(4), 86.9(2); Pt(2)–Sn(2)–Cl(6), 114.9(5); Pt(2)–Sn(2)–Cl(7), 118.8(9); Pt(2)–Sn(2)–Cl(8), 122.3(8); Pt(2)–Sn(2)–Cl(6a), 117(1); Pt(2)–Sn(2)–Cl(7a), 118(1); Pt(2)–Sn(2)–Cl(8a), 126(1); Pt(2)–Sn(2)–Cl(6b), 116.1(9); Pt(2)–Sn(2)–Cl(7b), 118.8(7); Pt(2)–Sn(2)–Cl(8b), 122.2(9); Cl(6)–Sn(2)–Cl(7), 93(1); Cl(6)–Sn(2)–Cl(8), 101(1); Cl(7)–Sn(2)–Cl(8), 101(1); Cl(6a)–Sn(2)–Cl(7a), 92(2); Cl(6a)–Sn(2)–Cl(8a), 93(2); Cl(7a)–Sn(2)–Cl(8a), 98(2); Cl(6b)–Sn(2)–Cl(7b), 91(1); Cl(6b)–Sn(2)–Cl(8b), 97(1); Cl(7b)–Sn(2)–Cl(8b), 106(2). P(3)–Pt(2)–P(4)–C(47), 135.2(9); P(3)–Pt(2)–P(4)–C(53), −98.0(8); P(4)–Pt(2)–P(3)–C(35), 126.0(9); P(4)–Pt(2)–P(3)–C(41), −111.9(8).

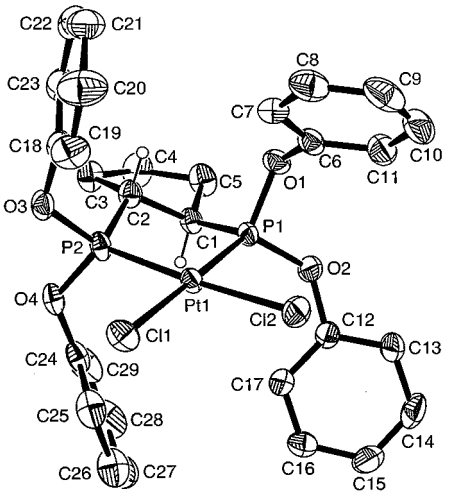

Fig. 10. Molecular structure of one of the two crystallographically independent molecules of $[(R,R)\text{-}C_5H_8\{P(OPh)_2\}_2PtCl_2]$, **(*R*,*R*)-3**. Selected bond lengths (Å) and valence and torsion angles (°): Pt(1)–Cl(1), 2.358(3); Pt(1)–Cl(2), 2.327(3); Pt(1)–P(1), 2.194(3); Pt(1)–P(2), 2.204(3). Cl(1)–Pt(1)–Cl(2), 89.8(1); Cl(1)–Pt(1)–P(1), 178.4(1); Cl(1)–Pt(1)–P(2), 92.2(1); Cl(2)–Pt(1)–P(1), 91.6(1); Cl(2)–Pt(1)–P(2), 176.6(2); P(1)–Pt(1)–P(2), 86.4(1). P(1)–Pt(1)–P(2)–O(3), −129.4(4); P(1)–Pt(1)–P(2)–O(4), 113.6(4); P(2)–Pt(1)–P(1)–O(1), 97.1(4); P(2)–Pt(1)–P(1)–O(2), −139.8(5). — Corresponding distances and angles for molecule 2: Pt(2)–Cl(3), 2.333(3); Pt(2)–Cl(4), 2.365(3); Pt(2)–P(3), 2.200(3); Pt(2)–P(4), 2.199(3). Cl(3)–Pt(2)–Cl(4), 90.0(1); Cl(3)–Pt(2)–P(3), 176.3(2); Cl(3)–Pt(2)–P(4), 91.6(1); Cl(4)–Pt(2)–P(3), 92.4(1); Cl(4)–Pt(2)–P(4), 178.4(1); P(3)–Pt(2)–P(4), 86.1(1). P(3)–Pt(2)–P(4)–O(7), −138.4(5); P(3)–Pt(2)–P(4)–O(8), 99.1(4); P(4)–Pt(2)–P(3)–O(5), −132.4(4); P(4)–Pt(2)–P(3)–O(6), 110.0(4).

significantly from the corresponding structural parameters that were previously derived from an X-ray structure determination of a racemic crystal of **3** (monoclinic $P2_1/n$) [13d]. This is particularly obvious for the Pt–Cl bonds, which in either crystallographically-independent molecule of the two **(*R*,*R*)-3** and **(*S*,*S*)-3** enantiomers differ by 0.030 Å (2.325(3)–2.331(3) vs. 2.358(3)–2.365(3) Å) but are averaged to 2.346(2) Å in structure **3** made up of equal proportions of the mirror image isomers. Averaging of structural parameters on going from either **(*R*,*R*)-3** or **(*S*,*S*)-3** to racemic **3** is, inter alia, also evident from the *trans* P–Pt–Cl angles which are different in the two enantiomorphous crystals (176.1(2)–176.6(2) vs. 178.2(1)–178.4(1)°) but are balanced out to 177.60(8)° in the centrosymmetric structure of the racemic specimen [13d]. The perspective views of the structural models given in Figs. 10 and 11 identify the puckering of the chelate rings in the λ,δ notation as λ for the *R*,*R*- and δ for the *S*,*S*-configured enantiomer. In either isomer the two phenoxy substituents belonging to the $P(OPh)_2$ groups *cis* to the shorter Pt–Cl bond exhibit distinct differences in the axial–equatorial character of their orientation relative to the coordination plane. Thus, the P–Pt–P–O torsion angles for the equatorially-aligned substituents amount to −138.4(5) and −139.8(5)° in the two independent molecules of **(*R*,*R*)-3** and, respectively, to 138.3(5) and 140.3(5)° for **(*S*,*S*)-3**, the corresponding torsion angles for the axially oriented groups being 99.1(4)°/97.1(4)° for the *R*,*R* enantiomer and −98.6(4)°/−97.0(4)° for the *S*,*S* form. While the orientation of the phenyl rings in the equatorial phenoxy substituents, relative to the $PtCl_2$ fragments of the molecules, can be described as 'face-on', the phenyl rings in the axially aligned phenoxy groups and the plane spanned by the metal and the chloro ligands are inclined to each other in a more parallel fashion such that these phenyl substituents appear to 'roof in' part of the coordination plane. Less pronounced differentiation between an axial or equatorial disposition is evident for the remaining two phenoxy groups, where the P–Pt–P–O torsion angles vary between 110.0(4)°/113.6(4)° and −132.4(4)°/−129.4(4)° in structure **(*R*,*R*)-3** and −109.7(5)°/−113.2(5)° and 132.5(5)°/130.4(4)° in complex **(*S*,*S*)-3**. These substituents are seen to contain their phenyl rings 'edge-on'-oriented in direction of, and away from, the $PtCl_2$ moieties.

To probe the above complexes for their enantioselectivity in the asymmetric hydroformylation of styrene, compounds **(*R*,*R*)-3**, **(*S*,*S*)-3**, and **(*S*,*S*)-4** were combined with $SnCl_2$ and the olefin in toluene under the

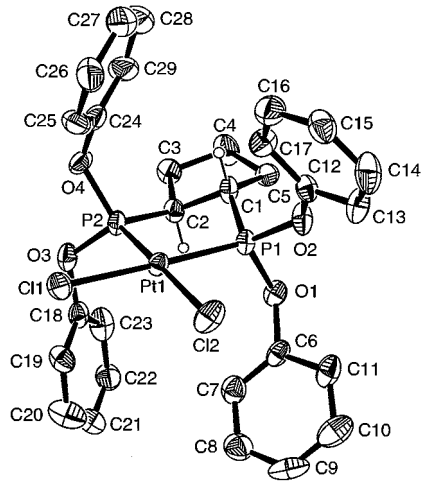

Fig. 11. Molecular structure of one of the two crystallographically independent molecules of $[(S,S)\text{-}C_5H_8\{P(OPh)_2\}_2PtCl_2]$, **(*S*,*S*)-3**. Selected bond lengths (Å) and valence and torsion angles (°): Pt(1)–Cl(1), 2.360(3); Pt(1)–Cl(2), 2.325(3); Pt(1)–P(1), 2.207(3); Pt(1)–P(2), 2.205(3). Cl(1)–Pt(1)–Cl(2), 89.6(1); Cl(1)–Pt(1)–P(1), 178.2(1); Cl(1)–Pt(1)–P(2), 92.3(1); Cl(2)–Pt(1)–P(1), 92.0(1); Cl(2)–Pt(1)–P(2), 176.1(1); P(1)–Pt(1)–P(2), 86.1(1). P(1)–Pt(1)–P(2)–O(3), 130.4(5); P(1)–Pt(1)–P(2)–O(4), −113.2(5); P(2)–Pt(1)–P(1)–O(1), −97.0(4); P(2)–Pt(1)–P(1)–O(2), 140.3(5). — Corresponding distances and angles for molecule 2: Pt(2)–Cl(3), 2.331(3); Pt(2)–Cl(4), 2.362(3); Pt(2)–P(3), 2.200(3); Pt(2)–P(4), 2.196(4). Cl(3)–Pt(2)–Cl(4), 90.3(1); Cl(3)–Pt(2)–P(3), 176.2(2); Cl(3)–Pt(2)–P(4), 91.3(1); Cl(4)–Pt(2)–P(3), 92.1(1); Cl(4)–Pt(2)–P(4), 178.4(1); P(3)–Pt(2)–P(4), 86.4(1). P(3)–Pt(2)–P(4)–O(7), 138.3(5); P(3)–Pt(2)–P(4)–O(8), −98.6(4); P(4)–Pt(2)–P(3)–O(5), 132.5(5); P(4)–Pt(2)–P(3)–O(6), −109.7(5).

Table 6
Asymmetric styrene hydroformylation catalyzed by complexes **(*R*,*R*)-3**, **(*S*,*S*)-3**, and **(*S*,*S*)-4**

T (°C)	*p*(CO) (bar)	*p*(H_2) (bar)	Time (h)	Conversion (%)	Aldehydes (%)	*b*/*n* ratio	*e.e.* (%) (configuration)	Ethylbenzene (%)
(*R*,*R*)-3								
80	40	40	13	100	69	64:36	0.7 (*S*)	28 [a]
(*S*,*S*)-3								
40	40	40	13	100	79	53:47	0.7 (*S*)	21
60	40	40	13	100	72	66:34	0.6 (*R*)	28
80	40	40	13	100	68	66:34	0.6 (*R*)	29 [a]
(*S*,*S*)-4								
80	20	60	24	100	70	65:35	9.1 (*R*)	30
80	40	40	24	100	75	67:33	17.7 (*R*)	25

0.013 mmol of Pt complex, 0.025 mmol of $SnCl_2$, and 2.2 mmol of styrene in 3 ml of [D_8]toluene.
[a] Approximately 3% of 3-phenylpropanol was also detected.

usual conditions (Pt complex–$SnCl_2$–substrate = 1:2:170; $T = 80$ °C; $p(H_2) = p(CO) = 40$ bar). Accepting inevitably low regioisomeric excesses of the branched aldehyde, the reaction mixtures were depressurized after 13–24 h in order to suppress the consecutive hydrogenation of the primary hydroformylation products. With the phenoxy-substituted systems **(*R*,*R*)-3** and **(*S*,*S*)-3** as catalyst precursors, practically null enantiomeric excesses were found, even if the temperature was decreased to 40 °C (Table 6). While this could be explained by an only limited rigidity of the $C_5H_8[P(OPh)_2]_2$ ligand bearing phenoxy substituents which can swivel about the P–O–C-hinges, use of the much more rigid P–C-bonded chelate phosphane $C_5H_8(PPh_2)_2$ as steering ligand in the **(*S*,*S*)-4**/$SnCl_2$ catalyst also resulted in discouraging low enantioselectivities of, at best, 18%. Hence, intrinsic ligand properties (in this case, any well or less well defined spatial orientation of the donor groups) once more do not seem to contribute to a significant extent to the catalytic outcome of the $[C_5H_8(PR_2)_2Pt(X)(Y)]$-catalyzed hydroformylation of styrene. The low optical yields obtained with platinum complexes of the respective $C_5H_8[P(OPh)_2]_2$ and $C_5H_8(PPh_2)_2$ enantiomers most probably also reflect the presence of different catalytic intermediates and cannot be attributed only to extensive racemization of the branched aldehyde as a consequence of reaction time and temperature, because racemization should be slow at 40–60 °C [20d].

2.4. Styrene hydroformylation using a $[C_5H_8(PPh_2)_2Pt(CH_3)(OSO_2CF_3)]$–$SnCl_2$ catalyst

In the absence of added $SnCl_2$, triflate complex **11** showed little hydroformylation activity. Thus, at a platinum-to-olefin ratio of 1:85, less than 20% styrene conversion was effected in toluene at 80 °C under 50–80 bar of CO/H_2 (1:1) after 66 h. Although the chemoselectivity towards aldehydes was good ($\sim 90\%$) at these low conversions, the regioselectivity for the branched product was virtually worthless owing to the predominance of the normal aldehyde in the mixture (Table 7).

Adding two equivalents of tin(II) chloride to $[C_5H_8(PPh_2)_2Pt(CH_3)(OSO_2CF_3)]$ caused the performance of the catalytic system to change dramatically. Using a catalyst-to-substrate ratio of 1:170 and similar conditions as before, quantitative conversion of the styrene substrate was observed within 20–40 h. Due to extensive subsequent hydrogenation of the primary hydroformylation products, the total aldehyde yield of the reaction was, however, much lower than that given by the tin-free catalyst. Both in the aldehydes and in the alcohols, the selectivities for the branched products were relatively high but, concerning the propanals, inverse to those provided by tin-free **11** and, with regard to the propanols, inverse to those provided by platinum–tin catalysts derived from chloro-substituted complexes such as **3** and **4**.

With triflate complex **11** as catalyst precursor, the consecutive hydrogenation of the two isomeric aldehydes did not come unexpected, since previous work had shown that successive hydrogenation of the aldehyde regioisomers is also a feature of [{bis(phosphane)}$PtCl_2$]–$Sn(O_3SCF_3)_2$–$SnCl_2$ catalysts [20d] and [{bis(phosphane)}$Pt(C_2H_4)$] complexes activated by methanesulfonic acid [25a]. The distinct selectivity of $[C_5H_8(PPh_2)_2Pt(CH_3)(OSO_2CF_3)]$–$SnCl_2$ towards the formation of 2-phenylpropanol differs, however, from that reported for these earlier systems, which were shown to favor the production of the linear alcohol over that of the branched.

3. Conclusions

This work has shown that platinum complexes containing cyclopentane-based C_2 chiral bis(phosphane) and bis(phosphonite) ligands, $[C_5H_8(PPh_2)_2Pt(Cl)(X)]$ ($X = CH_3$, CH_2CMe_3), $[C_5H_8\{P(OPh)_2\}_2PtCl_2]$, and

Table 7
$[C_5H_8(PPh_2)_2Pt(CH_3)(OSO_2CF_3)]$-catalyzed styrene hydroformylation in the absence and presence of added tin(II) chloride

T (°C)	p (bar)	Time (h)	Conversion (%)	Total aldehyde yield (%)	Selectivity for 2-phenylpropanal	Total alcohol yield (%)	Selectivity for 2-phenylpropanol	Ethylbenzene yield (%)
No $SnCl_2$ added (complex–styrene = 1:85)								
80	50	66	10	~90	~20:80			~10
80	80	66	17	~90	~20:80			~10
2 equiv. of $SnCl_2$ added (complex–styrene = 1:170)								
80	80	36	100	6	[a]	75	77:23	19
80	80	20	100	49	94:6	32	75:25	19

0.013 mmol of Pt complex **11** and required amount of styrene in 3 ml of $[D_8]$toluene; $p(H_2) = p(CO)$.

[a] Not determined; practically no *n*-aldehyde detected by NMR.

$[C_5H_8(PPh_2)_2Pt(CH_3)(OSO_2CF_3)]$ are catalysts for the hydroformylation of styrene, if activated by $SnCl_2$. To our best knowledge, no application of bis(phosphonite)-containing transition metal complexes to the hydroformylation of prochiral substrates has ever been described before. The chemoselectivity to the formation of aldehydes at 100% conversion is, in general, relatively low because hydroformylation is always followed by hydrogenation of the initially produced propanals to the corresponding alcohols. With $[C_5H_8(PPh_2)_2Pt(Cl)(alkyl)]$–$SnCl_2$ (alkyl = CH_3, CH_2CMe_3) and $[C_5H_8\{P(OPh)_2\}_2PtCl_2]$–$SnCl_2$ as catalytic systems, the unbranched aldehyde undergoes consecutive reduction faster than the branched product, which accounts for the high regioselectivity towards the branched aldehyde (b/n ratios $\geq$ 91:9) that is observed at complete conversion of the styrene substrate. Irrespective of a rigid or less rigid substitution of the donor functions of the $C_5H_8(PR_2)_2$ ligands, only low enantiomeric excesses were found for selected catalysts bearing optically active $C_5H_8[P(OPh)_2]_2$ or $C_5H_8(PPh_2)_2$ chelate phosphanes. In view of the different catalytically active species probably involved in the competitive and consecutive hydroformylation and hydrogenation reactions that were observed for the systems studied, it seems unlikely that further modification of the cyclopentane-based supporting ligands of $[C_5H_8(PR_2)_2Pt(X)(Y)]$ complexes will give rise to significantly enhanced selectivities.

4. Experimental

4.1. General remarks

All manipulations were performed under nitrogen using standard Schlenk techniques. Solvents were distilled from the appropriate drying agents prior to use. — NMR: Bruker DPX 300 (300.1 MHz for ^{1}H, 75.5 MHz for ^{13}C, 282.4 MHz for ^{19}F, 121.5 MHz for ^{31}P, and 149.2 MHz for ^{119}Sn) at 20 ± 2 °C (if not stated otherwise) with $SiMe_4$ as internal or with $CFCl_3$, H_3PO_4 or $SnMe_4$ as external standards (downfield positive); estimated accuracy of couplings to ^{195}Pt and ^{117,119}Sn: ± 5 Hz; 'ΣJ(P,C)': separation of the two most intense lines in the various $^{13}C\{^1H\}$ AA′X or ABX multiplets. — Polarimetry: Perkin–Elmer PE 241(1 dm cells at room temperature (r.t.)); $[\alpha]_\lambda$ in 10 deg cm^2 g^{-1} (estimated accuracy: ± 3%), c in g 100 ml^{-1}. — Gas chromatography: Hewlett-Packard/Agilent Technologies GC 5890 II (split injection; Rt βDex cst column 30 m × 0.32 mm (Restek, Bad Homburg, Germany), film thickness 0.25 μm; carrier gas 70 kPa H_2; FID detector).

Tin(II) chloride (99.99 + %, Aldrich) was used as supplied. — The racemic ligands $C_5H_8(PR_2)_2$, where $PR_2 = PPh_2$, P(N-pip)$_2$, or P(OPh)$_2$, were prepared as previously described [12,13d]. Similar procedures were used for the synthesis of the enantiopure compounds (1R,2R)- and (1S,2S)-$C_5H_8(PR_2)_2$ (R = Ph, OPh) from the resolved enantiomers of *trans*-$C_5H_8(PCl_2)_2$ [13a,13c,13e]. As expected, the products exhibited NMR and MS data corresponding in all respects to those reported for the racemates. — Optical rotations (all c = 1, $CHCl_3$): (1R,2R)-$C_5H_8(PPh_2)_2$; $[\alpha]_{589}$ + 173, $[\alpha]_{578}$ + 182, $[\alpha]_{546}$ + 210, $[\alpha]_{436}$ + 398, $[\alpha]_{365}$ + 728. (1S,2S)-$C_5H_8(PPh_2)_2$; $[\alpha]_{589}$ − 171, $[\alpha]_{578}$ − 180, $[\alpha]_{546}$ − 208, $[\alpha]_{436}$ − 394, $[\alpha]_{365}$ − 721. (1R,2R)-$C_5H_8[P(OPh)_2]_2$; $[\alpha]_{589}$ − 50, $[\alpha]_{578}$ − 52, $[\alpha]_{546}$ − 60, $[\alpha]_{436}$ − 102, $[\alpha]_{365}$ − 160; (1S,2S)-$C_5H_8[P(OPh)_2]_2$; $[\alpha]_{589}$ + 50, $[\alpha]_{578}$ + 52, $[\alpha]_{546}$ + 59, $[\alpha]_{436}$ + 101, $[\alpha]_{365}$ + 160. — The 1,5-cyclooctadiene precursors [(1,5-C_8H_{12})Pt(Cl)(X)] (X = Cl [33a,33c], CH_3 [33b], CH_2CMe_3 [33d]), and the chelate complexes $[C_5H_8\{P(N\text{-pip})_2\}_2Pt(Cl)(CH_2CMe_3)]$ (**8**) and $[C_5H_8\{P(N\text{-pip})_2\}_2Pt(CH_2CMe_3)_2]$ (**10**) [13d] were prepared by the published procedures or slight modifications thereof. For compound **8**, completing NMR data are as follows: ^{1}H-NMR (CD_2Cl_2): δ = 1.03 (s; 9 H, CH_3) 1.35–2.20 (m; 32 H, CCH_2C and $PtCH_2C$), 2.49–2.62 (m; 2 H, CH), 3.03–3.58 (m; 16 H, NCH_2C). — $^{13}C\{^1H\}$-NMR ($CDCl_3$): δ = 22.13, 22.68 [both ABX-dd, ΣJ(P,C) = 22.5 Hz each; both 1 C_5H_8-$C^{3,5}H_2$], 23.81, 23.91, 23.98, 24.04 (all s; all 1 piperidino C^4H_2), 25.77, 25.83, 26.02, 26.14 [all d, ^3J(P,C) = 4.4 Hz each; all 2 piperidino $C^{3,5}H_2$], 28.74 [ABX-dd, ΣJ(P,C) = 18.2 Hz; C_5H_8-C^4H_2), 29.53 [dd, *trans*-^2J(P,C) = 117.0, *cis*-^2J(P,C) = 5.1 Hz, ^{195}Pt satellites not resolved; Pt$CH_2C(CH_3)_3$], 34.39 [^{195}Pt-flanked d, ^3J(P,C) = 2.2, ^2J(Pt,C) ≅ 14 Hz; $PtCH_2C(CH_3)_3$], 34.61 [^{195}Pt-flanked d, ^4J(P,C) = 5.8, ^3J(Pt,C) ≅ 30 Hz; $PtCH_2C(CH_3)_3$], 46.39 (s, 2 piperidino $C^{2,6}H_2$), 46.78 [ABX-dd, ΣJ(P,C) = 50.8 Hz; 1 C_5H_8-$C^{1,2}H$], 47.53 (s), 47.84 [^{195}Pt-flanked d, ^2J(P,C) = 5.1, ^3J(Pt,C) ≅ 17 Hz], 46.56 [^{195}Pt-flanked d, ^2J(P,C) = 5.1, ^3J(Pt,C) = 32.7 Hz] (all 2 piperidino $C^{2,6}H_2$], 55.78 [ABX-dd, ΣJ(P,C) = 85.0 Hz; 1 C_5H_8-$C^{1,2}H$].

4.2. Dichloro and alkylchloro complexes

4.2.1. $[C_5H_8(PPh_2)_2PtCl_2]$ (1)

A solution containing 650 mg (1.74 mmol) of [(1,5-C_8H_{12})$PtCl_2$] and 780 mg (1.78 mmol) of $C_5H_8(PPh_2)_2$ in 35 ml of dichloromethane was stirred at room temperature (r.t.) overnight. Evaporation of the solvent left the product as an off-white powder which was freed from any unreacted starting complex by trituration with hot acetone and subsequently washed with ethanol; yield 1.10 g (90%). — ^{1}H-NMR (CD_2Cl_2): δ = 1.14–2.12 (m; 6 H, CH_2), 2.75–2.85 (m; 2 H, CH), 7.39–7.92 (m; 20 H, C_6H_5). — $^{13}C\{^1H\}$-NMR (CD_2Cl_2): δ = 22.96 [filled-in AA′X-dd, ΣJ(P,C) = 13.1

Hz; 2 C_5H_8-$C^{3,5}H_2$], 31.31 [t, $^3J(P,C) = 8.7$ Hz; C_5H_8-C^4H_2], 48.31 [filled-in AA′*X*-dd, $\Sigma J(P,C) = 58.1$ Hz; 2 C_5H_8-$C^{1,2}H$], 124.74 [dd, $J(P,C) = 62.5$, 3.6 Hz], 127.34 [dd, $J(P,C) = 68.3$, 2.9 Hz] (both 2 C_6H_5 *ipso*-C), 129.52 [AA′*X*-qui, $\Sigma J(P,C) = 13.1$ Hz; 8 C_6H_5 *meta*-C], 132.53, 133.44 (both s; both 2 C_6H_5 *para*-C), 133.83 [AA′*X*-qui, $\Sigma J(P,C) = 9.4$ Hz], 137.43 [AA′*X*-qui, $\Sigma J(P,C) = 11.6$ Hz] (both 4 C_6H_5 *ortho*-C). — $^{31}P\{^1H\}$-NMR (CD_2Cl_2): $\delta = 16.7$ [^{195}Pt-flanked s, $^1J(Pt,P) = 3600$ Hz]. — Anal. Found: C, 49.40; H, 4.48. $C_{29}H_{28}Cl_2P_2Pt$ (704.5). Calc.: C, 49.44; H, 4.01%.

4.2.2. [$C_5H_8\{P(N\text{-}pip)_2\}_2PtCl_2$] (2)

The preparation was carried out as described for **1** by reacting 160 mg (0.43 mmol) of [(1,5-C_8H_{12})$PtCl_2$] with 200 mg (0.43 mmol) of $C_5H_8[P(N\text{-}pip)_2]_2$ in 10 ml of CH_2Cl_2. The crude product was washed with ethanol and diethyl ether (20 ml each) and purified further by crystallization from CH_2Cl_2–*n*-hexane; yield 240 mg (77%) of **2** as colorless crystals. — ^{1}H-NMR ($CDCl_3$): $\delta = 1.41$–1.86 (m; 30 H, CCH_2C), 2.47–2.59 (m; 2 H, CH), 3.09–3.60 (m; 16 H, NCH_2C). — $^{13}C\{^1H\}$-NMR ($CDCl_3$): $\delta = 21.14$ [AA′*X*-qui, $\Sigma J(P,C) = 15.3$ Hz; 2 C_5H_8-$C^{3,5}H_2$), 24.39, 24.59 (both s; both 2 piperidino C^4H_2), 26.30 [AA′*X*-t, $\Sigma J(P,C) \cong 25$ Hz], 26.67 (br s) (both 4 piperidino $C^{3,5}H_2$), 30.74 (s; C_5H_8-C^4H_2), 47.64, 48.42 (both s; both 4 piperidino $C^{2,6}H_2$), 49.9 [badly resolved AA′*X*-t; 2 C_5H_8-$C^{1,2}H$]. — $^{31}P\{^1H\}$-NMR ($CDCl_3$): $\delta = 68.5$ [^{195}Pt-flanked s, $^1J(Pt,P) = 4340$ Hz]. — Anal. Found: C, 41.01; H, 6.31; N, 7.36. $C_{25}H_{48}Cl_2N_4P_2Pt$ (732.6). Calc.: C, 40.99; H, 6.60; N, 7.65%.

4.2.3. rac-[$C_5H_8\{P(OPh)_2\}_2PtCl_2$] (3) and resolved enantiomers (R,R)-3 and (S,S)-3

This material, which was previously isolated in low yield from prolonged acidolysis with methanolic HCl of [$C_5H_8\{P(OPh)_2\}_2Pt(CH_2CMe_3)_2$] [13d], formed virtually quantitatively on combining [(1,5-C_8H_{12})$PtCl_2$] (730 mg, 1.95 mmol) with a slight excess of *rac*-$C_5H_8[P(OPh)_2]_2$ (990 mg, 1.97 mmol) in dichloromethane (15 ml) as detailed for **1**; yield (after trituration with acetone, followed by washing with ethanol and diethyl ether) 1.40 g (92%) as off-white microcrystals. — ^{1}H-NMR ($CDCl_3$): $\delta = 1.73$–2.14 (m; 6 H, CH_2), 2.51–2.58 (m; 2 H, CH), 7.13–7.41 (m; 20 H, C_6H_5). — $^{13}C\{^1H\}$-NMR ($CDCl_3$): $\delta = 21.51$ [filled-in AA′*X*-dd, $\Sigma J(P,C) = 15.3$ Hz; 2 C_5H_8-$C^{3,5}H_2$], 32.51 (s; C_5H_8-C^4H_2), 54.20 [filled-in AA′*X*-dd, $\Sigma J(P,C) = 82.1$ Hz; 2 C_5H_8-$C^{1,2}H$], 123.00, 123.31 (both s; both 4 C_6H_5 *meta*-C), 127.79, 127.81 (both s; both 2 C_6H_5 *para*-C), 131.50, 131.83 (both s; both 4 C_6H_5 *ortho*-C), 151.95 [AA′*X*-t, $\Sigma J(P,C) = 8.0$ Hz], 153.02 [AA′*X*-t, $\Sigma J(P,C) = 7.3$ Hz] (both 2 C_6H_5 *ipso*-C). — $^{31}P\{^1H\}$-NMR ($CDCl_3$): $\delta = 101.3$ [^{195}Pt-flanked s, $^1J(Pt,P) = 4640$ Hz]; ref. [13d]: $\delta(CDCl_3) = 98.9$ [$^1J(Pt,P) = 4657$ Hz]. — Anal. Found: C, 44.29; H, 3.55. $C_{29}H_{28}Cl_2O_4P_2Pt$ (768.5). Calc.: C, 45.33; H, 3.67%. — Samples of higher analytical purity were obtained, if *cis*-[$(Et_2S)_2PtCl_2$] [51] (560 mg, 1.26 mmol, in 20 ml of CH_2Cl_2) was used as starting material for the ligand exchange reaction with $C_5H_8[P(OPh)_2]_2$ (700 mg, 1.39 mmol); yield 900 mg (94%). — Found: C, 45.87; H, 3.61%. — With (1*R*,2*R*)- and (1*S*,2*S*)-$C_5H_8[P(OPh)_2]_2$ as chelating ligands, the optically pure enantiomers **(*R*,*R*)-3** and **(*S*,*S*)-3** were prepared by the same method. — Optical rotations (both $c = 1$, $CHCl_3$): **(*R*,*R*)-3**; $[\alpha]_{589}$ +165, $[\alpha]_{578}$ +174, $[\alpha]_{546}$ +201, $[\alpha]_{436}$ +384. **(*S*,*S*)-3**; $[\alpha]_{589}$ −166, $[\alpha]_{578}$ −175, $[\alpha]_{546}$ −202, $[\alpha]_{436}$ −383, $[\alpha]_{365}$ −717.

4.2.4. rac-[$C_5H_8(PPh_2)_2Pt(Cl)(CH_3)$] (4) and resolved enantiomers (R,R)-4 and (S,S)-4

A solution of 575 mg (1.31 mmol) of racemic $C_5H_8(PPh_2)_2$ in 20 ml of dichloromethane was added dropwise to a solution of 460 mg (1.30 mmol) of [(1,5-C_8H_{12})Pt(Cl)(CH_3)] in an equal volume of the same solvent. After 1 h at ambient temperature, all volatile material was removed under a dynamic vacuum to leave a solid residue which was purified by thorough trituration, first with ethanol (20 ml) and then with diethyl ether (20 ml); yield 620 mg (70%) of **4** as an off-white powder. — ^{1}H-NMR (CD_2Cl_2): $\delta = 0.43$ [^{195}Pt-flanked dd, $^3J(P,H) = 7.5$, 3.7, $^2J(Pt,H) = 57$ Hz; 3 H, $PtCH_3$], 1.17–2.07 (m; 6 H, CH_2), 2.39–2.89 (m; 2 H, CH), 7.42–7.90 (m; 20 H, C_6H_5). — $^{13}C\{^1H\}$-NMR (CD_2Cl_2): $\delta = 7.14$ [dd, *trans*-$^2J(P,C) = 94.5$, *cis*-$^2J(P,C) = 6.5$ Hz, ^{195}Pt satellites not resolved; $PtCH_3$], 22.64 [AB*X*-dd, $\Sigma J(P,C) = 10.9$ Hz], 22.90 [AB*X*-dd, $\Sigma J(P,C) = 12.3$ Hz] (both 1 C_5H_8-$C^{3,5}H_2$), 30.15 [badly resolved AB*X*-m; C_5H_8-C^4H_2], 44.71[AB*X*-dd, $\Sigma J(P,C) = 45.8$ Hz], 50.73 [AB*X*-dd, $\Sigma J(P,C) = 65.4$ Hz] (both 1 C_5H_8-$C^{1,2}H$), 124.62 [d, $^1J(P,C) = 58.1$ Hz; 1 C_6H_5 *ipso*-C], 128.0–128.6 (overlapping doublets; 8 C_6H_5 *meta*-C], 130.17, 130.85, 131.10, 131.69 [all d, $^4J(P,C) = 2.2$ Hz each; all 1 C_6H_5 *para*-C], 132.08 [d, $^2J(P,C) = 9.4$ Hz], 132.90 [d, $^2J(P,C) = 8.7$ Hz], 136.39 [d, $^2J(P,C) = 13.1$ Hz], 136.67 [d, $^2J(P,C) = 12.4$ Hz] (all 2 C_6H_5 *ortho*-C); remaining *ipso*-C resonances superimposed by *meta*-C signals. — $^{31}P\{^1H\}$-NMR (CD_2Cl_2): $\delta = 21.2$ [^{195}Pt-flanked d, $^{2+3}J(P,P) = 14$, $^1J(Pt,P) = 4255$ Hz; P *trans* Cl], 23.3 [^{195}Pt-flanked d, $^1J(Pt,P) = 1705$ Hz; P *trans* C]. — Anal. Found: C, 52.55; H 5.06. $C_{30}H_{31}ClP_2Pt$ (684.1). Calc.: C, 52.68; H 4.57%. — The optically active complexes **(*R*,*R*)-4** and **(*S*,*S*)-4** were obtained analogously by combining [(1,5-C_8H_{12})Pt(Cl)(CH_3)] with equimolar amounts of (1*R*,2*R*)- or (1*S*,2*S*)-$C_5H_8(PPh_2)_2$. — Optical rotations (both $c = 1$, $CHCl_3$): **(*R*,*R*)-4**; $[\alpha]_{589}$ −187, $[\alpha]_{578}$ −196, $[\alpha]_{546}$ −224, $[\alpha]_{436}$ −401, $[\alpha]_{365}$ −701. **(*S*,*S*)-4**; $[\alpha]_{589}$ +186, $[\alpha]_{578}$ +194, $[\alpha]_{546}$ +222, $[\alpha]_{436}$ +396, $[\alpha]_{365}$ +682.

*4.2.5. $[C_5H_8\{P(N\text{-}pip)_2\}_2Pt(Cl)(CH_3)]$ (**5**)*

A solution composed of 510 mg (1.44 mmol) of $[(1,5\text{-}C_8H_{12})Pt(Cl)(CH_3)]$ and 680 mg (1.46 mmol) of $C_5H_8[P(N\text{-pip})_2]_2$ in 30 ml of CH_2Cl_2 was stirred at r.t. overnight. The residue remaining after removal of all volatiles was washed with ethanol and diethyl ether (20 ml each) and subsequently crystallized from CH_2Cl_2 to give 720 mg (70%) of **5** as colorless crystals. — ^{1}H-NMR ($CDCl_3$): $\delta = 0.46$ [^{195}Pt-flanked dd, $^3J(P,H) = 8.4, 2.4$, $^2J(Pt,H) = 52$ Hz; 3 H, $PtCH_3$], 1.37–2.09 (m; 30 H, CCH_2C), 2.10–2.38 (m; 2 H, CH), 2.93–3.43 (m; 16 H, NCH_2C). — $^{13}C\{^{31}P,^1H\}$-NMR ($CDCl_3$): $\delta = 0.04$ (s, ^{195}Pt satellites not resolved; $PtCH_3$), 22.18, 22.90 (both s; both 1 C_5H_8-$C^{3,5}H_2$), 24.78, 24.89, 24.91, 25.01 (all s; all 1 piperidino C^4H_2), 26.59, 26.88, 26.97, 27.18 (all s; all 2 piperidino $C^{3,5}H_2$), 30.19 (s; C_5H_8-C^4H_2), 47.53, 47.98, 48.98, 49.16 (all s; all 2 piperidino $C^{2,6}H_2$), 49.33, 53.62 (both s; both 1 C_5H_8-$C^{1,2}H$). — $^{31}P\{^1H\}$-NMR ($CDCl_3$): $\delta = 78.4$ [^{195}Pt-flanked d, $^{2+}3J(P,P) = 17$, $^1J(Pt,P) = 5000$ Hz; P *trans* Cl], 106.0 [^{195}Pt-flanked d, $^1J(Pt,P) = 2215$ Hz; P *trans* C]. — Anal. Found: C, 43.59; H, 7.76; N, 7.60. $C_{26}H_{51}ClN_4P_2Pt$ (712.2). Calc.: C, 43.85; H, 7.22; N, 7.87%.

*4.2.6. $[C_5H_8\{P(OPh)_2\}_2Pt(Cl)(CH_3)]$ (**6**)*

The complex was prepared as described for **5** by reacting 840 mg (2.37 mmol) of $[(1,5\text{-}C_8H_{12})Pt(Cl)(CH_3)]$ with 1.20 g (2.4 mmol) of $C_5H_8[P(OPh)_2]_2$ in 30 ml of dichloromethane; yield (after washing with ethanol and diethyl ether) 1.15 g (65%) of **6** as an off-white powder. — ^{1}H-NMR ($CDCl_3$): $\delta = 0.07$ [^{195}Pt-flanked dd, $^3J(P,H) = 9.8, 2.3$, $^2J(Pt,H) = 52$ Hz; 3 H, $PtCH_3$], 1.38–2.14 (m; 6 H, CH_2), 2.37–2.42 (m; 2 H, CH), 6.95–7.35 (m; 20 H, C_6H_5). — $^{13}C\{^1H\}$-NMR ($CDCl_3$): $\delta = 1.91$ [dd, *trans*-$^2J(P,C) = 123.6$, *cis*-$^2J(P,C) = 4.4$ Hz, ^{195}Pt satellites not resolved; $PtCH_3$], 19.81 [dd, $J(P,C) = 19.6, 5.9$ Hz], 20.55 [dd, $J(P,C) = 19.7, 6.3$ Hz] (both 1 C_5H_8-$C^{3,5}H_2$), 29.73 [AB*X*-dd, $\Sigma J(P,C) = 18.8$ Hz; C_5H_8-C^4H_2], 53.98 [dd, $J(P,C) = 37.8, 13.8$ Hz], 54.25 [dd, $J(P,C) = 66.1, 22.3$ Hz] (both 1 C_5H_8-$C^{1,2}H$), 120.56 [d, $^3J(P,C) = 5.1$ Hz], 120.86 [d, $^3J(P,C) = 5.2$ Hz], 121.50 [d, $^3J(P,C) = 3.7$ Hz], 122.25 [d, $^3J(P,C) = 3.8$ Hz] (all 2 C_6H_5 *ortho*-C), 125.10 (s), 125.29 [d, $^5J(P,C) = 1.4$ Hz], 125.50 [d, $^5J(P,C) = 1.5$ Hz], 125.76 [d, $^5J(P,C) = 2.1$ Hz] (all 1 C_6H_5 *para*-C), 129.7–129.9 (overlapping doublets; 8 C_6H_5 *meta*-C), 151.53 [AB*X*-d, $\Sigma J(P,C) = 8.0$ Hz], 151.86 [AB*X*-d, $\Sigma J(P,C) = 3.9$ Hz], 151.99 (deceptively simple s, $\Sigma J(P,C) \cong 0$ Hz], 152.68 [AB*X*-d, $\Sigma J(P,C) = 2.2$ Hz] (all 1 C_6H_5 *ipso*-C). — $^{31}P\{^1H\}$-NMR ($CDCl_3$): $\delta = 112.0$ [^{195}Pt-flanked d, $^{2+3}J(P,P) = 7$, $^1J(Pt,P) = 5635$ Hz; P *trans* Cl], 155.1 [^{195}Pt-flanked d, $^1J(Pt,P) = 2140$ Hz; P *trans* C]. — Anal. Found: C, 48.09; H, 4.07. $C_{30}H_{31}ClO_4P_2Pt$ (748.1). Calc.: C, 48.17; H, 4.18%.

*4.2.7. rac-$[C_5H_8(PPh_2)_2Pt(Cl)(CH_2CMe_3)]$ (**7**) and resolved enantiomers **(R,R)-7** and **(S,S)-7***

$[(1,5\text{-}C_8H_{12})Pt(Cl)(CH_2CMe_3)]$ (390 mg; 0.96 mmol) and 420 mg (0.96 mmol) of *rac*-$C_5H_8(PPh_2)_2$ were reacted in 15 ml of CH_2Cl_2 as delineated for **5**; yield (after crystallization from CH_2Cl_2–*n*-pentane) 470 mg (66%) of **7** as colorless crystals. — ^{1}H-NMR (CD_2Cl_2): $\delta = 0.69$ (s; 9 H, CH_3), 1.11–2.27 (m; 8 H, CH_2), 2.71–2.90 (m; 2 H, CH), 7.35–7.87 (m; 20 H, C_6H_5). — $^{13}C\{^1H\}$-NMR ($CDCl_3$): $\delta = 22.73$ [AB*X*-t, $\Sigma J(P,C) = 13.1$ Hz], 23.07 [AB*X*-t, $\Sigma J(P,C) = 10.9$ Hz] (both 1 C_5H_8-$C^{3,5}H_2$), 29.58 [AB*X*-dd, $\Sigma J(PC) = 15.3$ Hz; C_5H_8-C^4H_2], 34.83 [^{195}Pt-flanked d, $^4J(P,C) = 5.1$, $^3J(Pt,C) = 26.9$ Hz; $PtCH_2C(CH_3)_3$], 36.08 [^{195}Pt-flanked d, $^3J(P,C) = 2.2$, $^2J(Pt,C) \cong 13$ Hz; $PtCH_2C(CH_3)_3$], 40.00 [d, *trans*-$^2J(P,C) = 90.8$ Hz, *cis*-$^2J(P,C)$ not resolved, ^{195}Pt satellites not resolved; $PtCH_2C(CH_3)_3$], 42.30 [AB*X*-dd, $\Sigma J(P,C) = 41.4$ Hz], 51.54 [AB*X*-dd, $\Sigma J(P,C) = 66.9$ Hz] (both 1 C_5H_8-$C^{1,2}H$), 128.0–128.6 (overlapping doublets; 8 C_6H_5 *meta*-C), 130.07 (s; 1 C_6H_5 *para*-C), 130.84 [d, $^4J(P,C) = 2.2$ Hz; 2 C_6H_5 *para*-C], 131.91 [d, $^4J(P,C) = 2.2$ Hz; 1 C_6H_5 *para*-C], 132.65, 133.12 [both d, $^2J(P,C) = 9.4$ Hz each; both 2 C_6H_5 *ortho*-C], 136.14 [d, $^2J(P,C) = 12.4$ Hz; 2 C_6H_5 *ortho*-C], 136.88 [^{195}Pt-flanked d, $^2J(P,C) = 11.6$, $^3J(Pt,C) = 45.8$ Hz; 2 C_6H_5 *ortho*-C]; *ipso*-C resonances partially obscured by overlapping *meta*-C doublets. — $^{31}P\{^1H\}$-NMR (CD_2Cl_2): $\delta = 19.9$ [^{195}Pt-flanked *A*B-d, $^{2+3}J(P,P) = 14$, $^1J(Pt,P) = 4495$ Hz; P *trans* Cl], 20.4 [^{195}Pt-flanked A*B*-d, $^1J(Pt,P) = 1495$ Hz; P *trans* C]. — Anal. Found: C, 55.39; H, 5.63. $C_{34}H_{39}ClP_2Pt$ (740.1). Calc.: C, 55.17; H, 5.31%. — Virtually the same procedures were employed for the synthesis of the enantiopure complexes **(*R*,*R*)-7** and **(*S*,*S*)-7**. — Optical rotations: **(*R*,*R*)-7**; $[\alpha]_{589}$ −146, $[\alpha]_{578}$ −153, $[\alpha]_{546}$ −175, $[\alpha]_{436}$ −323 ($c = 1$, $CHCl_3$). **(*S*,*S*)-7**; $[\alpha]_{589}$ +138, $[\alpha]_{578}$ +145, $[\alpha]_{546}$ +169, $[\alpha]_{436}$ +304 ($c = 1$, $CHCl_3$); $[\alpha]_{589}$ +137, $[\alpha]_{578}$ +144, $[\alpha]_{546}$ +167, $[\alpha]_{436}$ +305, $[\alpha]_{365}$ +581 ($c = 0.5$, CH_2Cl_2).

*4.2.8. $[C_5H_8\{P(OPh)_2\}_2Pt(Cl)(CH_2CMe_3)]$ (**9**)*

This complex was originally obtained by controlled protolytic cleavage of the metal–carbon bond of the dineopentyl $[C_5H_8\{P(OPh)_2\}_2Pt(CH_2CMe_3)_2]$ [13d]. Alternatively, it can be prepared by combining $[(1,5\text{-}C_8H_{12})Pt(Cl)(CH_2CMe_3)]$ (440 mg, 1.08 mmol) with $C_5H_8[P(OPh)_2]_2$ (550 mg, 1.09 mmol) in dichloromethane (15 ml, r.t., overnight). Removal of all volatiles, followed by stirring the residue under ethanol (20 ml) afforded 690 mg (79%) of the product as colorless microcrystals. — ^{1}H-NMR (CD_2Cl_2): $\delta = 0.78$ (s; 9 H, CH_3), 1.96–1.24 (m; 8 H, CH_2), 2.28–2.31 (m; 2 H, CH), 7.15–7.44 (m; 20 H, C_6H_5). — $^{13}C\{^1H\}$-NMR ($CDCl_3$): $\delta = 19.25$ [dd, $J(P,C) = 18.2, 5.1$ Hz], 21.60 [dd, $J(P,C) = 18.2, 7.3$ Hz] (both 1

C_5H_8-$C^{3,5}H_2$), 29.38 [AB*X*-dd, ΣJ(P,C) = 17.6 Hz; C_5H_8-C^4H_2], 34.37 [dd, *trans*-^2J(P,C) = 122.8, *cis*-^2J(P,C) = 3.6 Hz, ^{195}Pt satellites not resolved; Pt$CH_2C(CH_3)_3$], 34.53 [^{195}Pt-flanked d, ^4J(P,C) = 8.3, ^3J(Pt,C) = 26.3 Hz; $PtCH_2C(CH_3)_3$], 35.58 [^{195}Pt-flanked d, ^3J(P,C) = 2.2, ^2J(Pt,C) ≅ 16 Hz; $PtCH_2C(CH_3)_3$], 53.73 [dd, J(P,C) = 33.4, 12.3 Hz], 54.16 [dd, J(P,C) = 59.6, 22.8 Hz] (both 1 C_5H_8-$C^{1,2}H$), 120.64 [d, ^3J(P,C) = 4.4 Hz], 120.91 [d, ^3J(P,C) = 4.4 Hz], 121.14 [d, ^3J(P,C) = 5.1 Hz], 121.84 [d, ^3J(P,C) = 3.6 Hz] (all 2 C_6H_5 *ortho*-C), 124.97, 125.08, 125.26, 125.53 [all d, ^5J(P,C) = 1.4 Hz each; all 1 C_6H_5 *para*-C), 129.5–129.9 (overlapping doublets; 8 C_6H_5 *meta*-C), 151.80 [AB*X*-d, ΣJ(P,C) = 10.9 Hz], 152.02 [AB*X*-d, ΣJ(P,C) = 3.7 Hz], 152.18 (AB*X*-d, ΣJ(P,C) = 12.3 Hz], 152.67 [AB*X*-d, ΣJ(P,C) = 2.9 Hz] (all 1 C_6H_5 *ipso*-C). — ^{31}P{^{1}H}-NMR (CD_2Cl_2): δ = 107.4 [^{195}Pt-flanked d, ^{2+3}J(P,P) = 8, ^1J(Pt,P) = 6085 Hz; P *trans* Cl], 156.6 [^{195}Pt-flanked d, ^1J(Pt,P) = 1905 Hz; P *trans* C]; ref. [13d]: δ(C_6D_6) = 105.0 [^{2+3}J(P,P) = 11, ^1J(Pt,P) = 6142 Hz], 164.5 [^1J(Pt,P) = 1905 Hz]. — Anal. Found: C, 50.76; H, 5.16. $C_{34}H_{39}ClO_4P_2Pt$ (804.1). Calc.: C, 50.78; H, 4.89%.

4.3. Triflate derivatives

4.3.1. [$C_5H_8(PPh_2)_2Pt(CH_3)(OSO_2CF_3)$] (**11**)

AgO_3SCF_3 (155 mg; 0.60 mol) was suspended in 20 ml of dichloromethane in the dark. A solution of 410 mg (0.60 mmol) of [$C_5H_8(PPh_2)_2Pt(Cl)(CH_3)$] (**4**) in 30 ml CH_2Cl_2 was added dropwise within 45 min and the resulting mixture was stirred for an additional 30 min at ambient conditions. Precipitated silver chloride was removed by filtration over Celite and the concentrated filtrate was diluted with *n*-pentane. The product separated from solution as an off-white solid which was collected after allowing the mixture to stand overnight at −20 °C in order to complete precipitation; yield 300 mg (63%). — ^{1}H-NMR (CD_2Cl_2): δ = 0.48 [^{195}Pt-flanked dd, ^3J(P,H) = 7.7, 1.6, ^2J(Pt,H) = 45 Hz; 3 H, $PtCH_3$], 1.12–2.07 (m; 6 H, CH_2), 2.44–2.60 (m; 2 H, CH), 7.40–7.98 (m; 20 H, C_6H_5). — ^{19}F{^{1}H}-NMR ($CDCl_3$): δ = −77.88 (s). — ^{31}P{^{1}H}-NMR (CD_2Cl_2): δ = 17.3 [^{195}Pt-flanked d, ^{2+3}J(P,P) = 13, ^1J(Pt,P) = 4975 Hz; P *trans* O], 34.3 [^{195}Pt-flanked d, ^1J(Pt,P) = 1810 Hz; P *trans* C]. — Anal. Found: C, 47.07; H, 3.79; S, 3.76. $C_{31}H_{31}F_3O_3P_2PtS$ (797.7). Calc.: C, 46.68; H, 3.92; S, 4.02%.

4.3.2. [$C_5H_8\{P(OPh)_2\}_2Pt(CH_3)(OSO_2CF_3)$] (**12**)

Silver triflate (100 mg; 0.38 mmol) and 290 mg (0.38 mmol) of [$C_5H_8\{P(OPh)_2\}_2Pt(Cl)(CH_3)$] (**6**) were allowed to interact in 40 ml of dichloromethane as described for **11**. The product was isolated from the filtered solution by removal of all volatile material; yield 260 mg (77%) of **12** as an off-white powder. — ^{1}H-NMR ($CDCl_3$): δ = 0.16 [^{195}Pt-flanked d, ^3J(P,H) = 9.8, ^2J(Pt,H) = 42 Hz; 3 H, $PtCH_3$], 1.30–2.22 (m; 6 H, CH_2), 2.43–2.69 (m; 2 H, CH), 7.11–7.44 (m; 20 H, C_6H_5). — ^{13}C{^{1}H}-NMR (CD_2Cl_2): δ = 1.88 [^{195}Pt-flanked dd, *trans*-^2J(P,C) = 111.2, *cis*-^2J(P,C) = 3.6, ^1J(Pt,C) = 440 Hz; $PtCH_3$], 19.64, 20.27 [both dd, J(P,C) = 18.9, 5.8 Hz each; both 1 C_5H_8-$C^{3,5}H_2$], 28.50 [AB*X*-dd, ΣJ(P,C) = 20.3 Hz; C_5H_8-C^4H_2], 119.23 [d, ^3J(P,C) = 5.8 Hz], 119.76 [d, ^3J(P,C) = 5.1 Hz] (both 2 C_6H_5 *ortho*-C), 120.60 (AB*X*-t, ΣJ(P,C) = 4.4 Hz; 4 C_6H_5 *ortho*-C), 124.63 (s; 1 C_6H_5 *para*-C), 125.16 (s; 2 C_6H_5 *para*-C), 125.54 (d, ^5J(P,C) = 2.2 Hz; 1 C_6H_5 *para*-C), 129.2, 129.4 (both overlapping doublets; 2 + 6 C_6H_5 *meta*-C), 150.36 [AB*X*-d, ΣJ(P,C) = 8.7 Hz], 150.96 [AB*X*-d, ΣJ(P,C) = 9.4 Hz], 151.20 (AB*X*-d, ΣJ(P,C) = 15.3 Hz], 152.34 [AB*X*-d, ΣJ(P,C) = 2.9 Hz] (all 1 C_6H_5 *ipso*-C); CH resonances obscured by solvent signal; CF_3 not detected. — ^{31}P{^{1}H}-NMR (CD_2Cl_2): δ = 99.5 [^{195}Pt-flanked d, ^{2+3}J(P,P) = 11, ^1J(Pt,P) = 6565 Hz; P *trans* O], 164.7 [^{195}Pt-flanked d, ^1J(Pt,P) = 2245 Hz; P *trans* C]. — Anal. Found: C, 43.47; H, 3.74; S, 3.67. $C_{31}H_{31}F_3O_7P_2PtS$ (861.7). Calc.: C, 43.21; H, 3.63; S, 3.72%.

4.3.3. [$C_5H_8(PPh_2)_2Pt(CH_2CMe_3)(OSO_2CF_3)$] (**13**)

A solution of 280 mg (0.38 mmol) of [$C_5H_8(PPh_2)_2Pt(Cl)(CH_2CMe_3)$] (**7**) in CH_2Cl_2 was stirred with 98 mg (0.38 mmol) of AgO_3SCF_3 for 2.5 h at r.t. in the dark. Silver chloride was filtered off over Celite and the filtrate was evaporated to dryness to leave 140 mg (43%) of **13** as a beige solid. — ^{1}H-NMR (CD_2Cl_2): δ = 0.69 (s; 9 H, CH_3), 0.95–2.40 (m; 8 H, CH_2), 2.76–2.94 (m; 2 H, CH), 7.40–7.92 (m; 20 H, C_6H_5). — ^{31}P{^{1}H}-NMR (CD_2Cl_2): δ = 15.2 [^{195}Pt-flanked d, ^{2+3}J(P,P) = 13, ^1J(Pt,P) = 5310 Hz; P *trans* O], 31.0 [^{195}Pt-flanked d, ^1J(Pt,P) = 1615 Hz; P *trans* C]. — Anal. Found (after recrystallization from ethanol): C, 49.42; H, 4.65; S, 3.67. $C_{35}H_{39}F_3O_3P_2PtS$ (853.7). Calc.: C, 49.24; H, 4.60; S, 3.76%.

4.3.4. [μ-$Cl\{C_5H_8(PPh_2)_2PtCH_3\}_2]O_3SCF_3$ (**14**)

At −60 °C, 60 mg (0.23 mmol) of AgO_3SCF_3 was added to a solution of 155 mg (0.23 mmol) of [$C_5H_8(PPh_2)_2Pt(Cl)(CH_3)$] (**4**) in 20 ml of CH_2Cl_2. After warming to r.t., the mixture was stirred for 1 h in the dark, filtered over Celite and evaporated. ^{31}P{^{1}H}-NMR spectroscopy showed the residual material to be a 3:1 mixture of products **11** and **14**. Crystallization of the solid from a dichloromethane–diethyl ether solvent mixture yielded colorless single-crystals of complex **14** as an addition compound containing 0.5 mol of lattice diethyl ether per formula unit, [μ-$Cl\{C_5H_8(PPh_2)_2PtCH_3\}_2]O_3SCF_3$·0.5 Et_2O (**14·0.5 Et_2O**). — ^{31}P{^{1}H}-NMR (CD_2Cl_2): δ = 21.11 [2 coinciding ^{195}Pt-flanked doublets, ^{2+3}J(P,P) = 13, ^1J(Pt,P) = 4625 Hz; 2 P *trans*

μ-Cl], 28.6 [^{195}Pt-flanked d, ^{1}J(Pt,P) = 1770 Hz], 29.0 [^{195}Pt-flanked d, ^{1}J(Pt,P) = 1760 Hz] (both 1 P *trans* C].

4.4. Trichlorostannato complexes [$C_5H_8(PPh_2)_2Pt(CH_3)(SnCl_3)$] (**15**), [$C_5H_8(PPh_2)_2Pt(Cl)(SnCl_3)$] (**16**), [$C_5H_8\{P(OPh)_2\}_2Pt(CH_3)(SnCl_3)$] (**17**), [$C_5H_8\{P(OPh)_2\}_2Pt(Cl)(SnCl_3)$] (**18**), [$C_5H_8(PPh_2)_2Pt(SnCl_3)_2$] (**19**), and [$C_5H_8\{P(OPh)_2\}_2Pt(SnCl_3)_2$] (**20**)

To 250 mg (0.37 mmol) of [$C_5H_8(PPh_2)_2Pt(Cl)(CH_3)$] (**4**) in 20 ml of acetone was added an equimolar quantity of anhydrous tin(II) chloride (70 mg). The resulting yellow solution was stirred for 10 min at r.t. and then reduced in volume. Layering with diethyl ether caused the deposition of crystals shown by $^{31}P\{^{1}H\}$-NMR as well as by an X-ray crystallographic study of a selected specimen (see below) to be a mixture of [$C_5H_8(PPh_2)_2Pt(CH_3)(SnCl_3)$], (**15**) ($\sim$52%), [$C_5H_8(PPh_2)_2Pt(Cl)(SnCl_3)$], (**16**) ($\sim$20%; crystal structure analysis), and [$C_5H_8(PPh_2)_2PtCl_2$], (**1**) ($\sim$28%). The identity of the latter two complexes was independently confirmed by combining equimolar amounts of **1** (150 mg, 0.21 mmol) and $SnCl_2$ (40 mg, 0.21 mmol) in 20 ml of CH_2Cl_2, which furnished the insertion product **12** together with unreacted dichloro complex **1** in the molar ratio 1:1. — **15**; ^{1}H-NMR ([D$_6$]acetone): $\delta = 0.59$ [^{195}Pt-flanked AB*X*-t, ΣJ(P,H) = 12.2, ^{2}J(Pt,H) = 59 Hz; 3 H, $PtCH_3$], 1.16–1.44, 1.76–1.89, 1.98–2.07 (all m; all 2 H, CH_2), 2.82–3.17 (m; 2 H, CH), 7.36–7.90 (m; 20 H, C_6H_5). — $^{31}P\{^{1}H\}$-NMR ($CDCl_3$): $\delta = 25.7$ [^{195}Pt-flanked d, ^{2+3}J(P,P) = 17, ^{1}J(Pt,P) = 1780 Hz; P *trans* C], 27.9 [^{195}Pt-flanked d, ^{1}J(Pt,P) = 3510 Hz; P *trans* Sn]; $^{2}J(^{117,119}$Sn,P) not resolved. — **16**; $^{31}P\{^{1}H\}$-NMR (CD_2Cl_2): $\delta = 18.1$ [^{195}Pt- and ^{117,119}Sn-flanked d, ^{2+3}J(P,P) = 11, ^{1}J(Pt,P) = 3353, *cis*-$^{2}J(^{117,119}$Sn,P) = 235 Hz; P *trans* Cl], 25.1 [d with ^{195}Pt, ^{117}Sn, and ^{119}Sn satellites, ^{1}J(Pt,P) = 3335, *trans*-$^{2}J(^{117}$Sn,P) = 3850, *trans*-$^{2}J(^{119}$Sn,P) = 4030 Hz; P *trans* Sn]; data from [$C_5H_8(PPh_2)_2PtCl_2$]–$SnCl_2$ reaction. — **1**; $^{31}P\{^{1}H\}$-NMR (CD_2Cl_2): $\delta = 17.3$ [^{195}Pt-flanked s, ^{1}J(Pt,P) = 3600 Hz]. — The reaction between [$C_5H_8\{P(OPh)_2\}_2Pt(Cl)(CH_3)$], **6** (200 mg, 0.26 mmol), and tin(II) chloride (50 mg, 0.26 mmol) in acetone (30 ml) was initially run at -20 °C. Evaporation of the solvent at this temperature left an orange–yellow residue which $^{119}Sn\{^{1}H\}$- and $^{31}P\{^{1}H\}$-NMR showed to be largely pure [$C_5H_8\{P(OPh)_2\}_2Pt(CH_3)(SnCl_3)$] (**17**), only slightly contaminated by traces of [$C_5H_8\{P(OPh)_2\}_2Pt(Cl)(SnCl_3)$] (**18**). Re-dissolution of this material in acetone at ambient temperature, followed by layering the mixture with *n*-hexane, resulted in the precipitation of a reddish solid containing [$C_5H_8\{P(OPh)_2\}_2Pt(CH_3)(SnCl_3)$], (**17**) ($\sim$56%), accompanied by [$C_5H_8\{P(OPh)_2\}_2Pt(Cl)(SnCl_3)$], (**18**) ($\sim$26%), and [$C_5H_8\{P(OPh)_2\}_2PtCl_2$], (**3**) ($\sim$18%). — **17**; $^{31}P\{^{1}H\}$-NMR ($CDCl_3$): $\delta = 127.3$ [^{195}Pt-flanked s (br), ^{1}J(Pt,P) = 4660 Hz; P *trans* Sn], 156.4 [^{195}Pt-flanked s (br), ^{1}J(Pt,P) = 2415 Hz; P *trans* C]; $^{2}J(^{117,119}$Sn,P) not resolved. — $^{119}Sn\{^{1}H\}$-NMR (CD_2Cl_2, -70 °C): $\delta = 52.9$ [dd with ^{195}Pt satellites, *trans*-$^{2}J(^{119}$Sn,P) = 4760, *cis*-$^{2}J(^{119}$Sn,P) = 295, ^{1}J(Pt,^{119}Sn) = 18870 Hz]. — **18**; $^{31}P\{^{1}H\}$-NMR ($CDCl_3$): $\delta = 110.5$ [^{195}Pt-flanked d, ^{2+3}J(P,P) = 18, ^{1}J(Pt,P) = 4455 Hz; P *trans* Cl], 120.8 [^{195}Pt-flanked d, ^{1}J(Pt,P) = 3830 Hz; P *trans* Sn]; $^{2}J(^{117,119}$Sn,P) not resolved. — **3**; $^{31}P\{^{1}H\}$-NMR ($CDCl_3$): $\delta = 101.0$ [^{195}Pt-flanked s, ^{1}J(Pt,P) = 4645 Hz]. — Thermal treatment of **4** and **6** (0.1 mmol each) with tin(II) chloride in 1:1 stoichiometry in toluene (20 ml) at 80 °C for 16–72 h yielded mixtures containing the dichloro complexes **1**/**3** together with the bis(trichlorostannates) [$C_5H_8(PR_2)_2Pt(SnCl_3)_2$] (R = Ph, **19**; OPh, **20**) as dominating products and the monotrichlorostannates **15**/**16** and **17**/**18** as minor constituents. — **19**; $^{31}P\{^{1}H\}$-NMR ($CDCl_3$): $\delta = 27.4$ [^{195}Pt- and ^{117,119}Sn- flanked s, ^{1}J(Pt,P) = 2515, *trans*-$^{2}J(^{117}$Sn,P) = 2005, *trans*-$^{2}J(^{119}$Sn,P) = 2095, *cis*-$^{2}J(^{117}$Sn,P) = 122, *cis*-$^{2}J(^{119}$Sn,P) = 166 Hz]. — **20**; $^{31}P\{^{1}H\}$-NMR ($CDCl_3$): $\delta = 143.8$ [^{195}Pt-flanked s, ^{1}J(Pt,P) = 3535 Hz]; $^{2}J(^{117,119}$Sn,P) not resolved.

4.5. Exemplary hydroformylation procedure

A 10-ml Schlenk tube equipped with a small magnetic stirring bar was charged with platinum catalyst (typically 0.012–0.013 mmol) and anhydrous tin(II) chloride ($\sim$0.025 mmol). [D_8]toluene (3 ml) and styrene (2.2 mmol) were added and the tube was inserted into an argon-filled 100-ml stainless steel autoclave. The autoclave was sealed, pressurized, and vented several times with a 1:1 CO/H_2 synthesis gas mixture (Messer Griesheim; 99.999% H_2, 99.997% CO) and subsequently pressurized (usually to 80 bar) and heated with stirring in an oil bath (typically at 80 °C). At the end of the reaction, the autoclave was cooled, the pressure was vented and the mixture of products was analyzed by ^{1}H-NMR spectroscopy. Conversions and product compositions were determined on the basis of the integrations of the PhC*H*=CH_2, PhC*H*(CH_3)CHO, PhCH_2-CH_2CHO, PhC*H*(CH_3)CH_2OH, PhCH_2CH_2CH_2OH, and PhCH_2CH_3 signals. The branched-to-normal ratios of the aldehydes were estimated by integrating the –CHO signals, $\delta \cong 9.2$ (t) for the normal and 9.3 (d) for the branched, those of the alcohols by comparing the intensities of the individual CH_2 and CH_3 resonances. Enantiomeric excesses were measured by gas chromatography following $NaBH_4$ reduction of the aldehydes to the corresponding alcohols. Absolute configurations were determined by comparing the retention times of the products with those of optically pure (*R*)-(−) and (*S*)-(+)-2-phenylpropanol.

4.6. X-Ray crystallographic studies

Single-crystals of the complexes studied by X-ray diffraction were grown from CH_2Cl_2–*n*-hexane (**2**), CH_2Cl_2–diethyl ether (**5**, **14·0.5 Et_2O**), CH_2Cl_2–*n*-pentane (**7**), acetone [**8**, **(*R*,*R*)-3**, **(*S*,*S*)-3**], methanol (**9**), acetone–THF (**10**), ethanol (**13**), and acetone–diethyl ether (**16**), respectively. The measurements were made at 20 ± 2 °C on a Nonius MACH 3 diffractometer using graphite-monochromated Mo–K_α radiation ($\lambda =$ 0.71073 Å): orientation matrices from the setting angles of 25 centered medium-angle reflections; collection of the diffraction intensities by ω scans; data corrected for absorption by ψ scans [52]. The structures were solved by direct methods and subsequently refined by full-matrix least-squares procedures on F^2 with allowance for anisotropic thermal motion of all non-hydrogen atoms employing the WinGX package [53] and the relevant programs (SIR-97 [54], SHELXL-97 [55], ORTEP-3 [56]) implemented therein. H atoms were included in the final structural models assuming ideal geometry and using appropriate riding models. According to the U_{ij} values of the symmetry-related CH carbon atoms of **10**, a twofold spatial disorder was suggested for these atoms, which was accounted for by assigning the carbon positions C(6a) and C(6b) split occupancies of 0.3 and 0.7, respectively. The ring carbon atoms of the binuclear cation of complex **14·0.5 Et_2O**, C(2)/C(2a), C(3)/C(3a), C(32)/C(32a), C(33)/C(33a) were similarly disordered over two sites with occupation factors of 0.5 each, so that the existence of the ion as a racemate or a *meso* compound could not be distinguished. The triflate anion of this structure showed positional disorder about its S–C axis which was resolved by employing occupancies of 0.6 for the first and 0.4 for the second anion and by restraining the two CF_3SO_3 groups so that their staggered conformations have 3*m* symmetry and are the same as each other. The Et_2O molecule of crystallization was only poorly defined and had to be refined with C–O and C–C bond lengths restrained to their ideal values. The trichlorostannate ligand attached to platinum atom Pt(2) in structure **16** displayed threefold rotational disorder about the Pt(2)–Sn(2) bond with occupancies of 0.45, 0.20, and 0.35 for the particular chlorine positions in the $–SnCl^{(6)}Cl^{(7)}Cl^{(8)}$, $–SnCl^{(6a)}Cl^{(7a)}Cl^{(8a)}$, and $–SnCl^{(6b)}Cl^{(7b)}Cl^{(8b)}$ groups.

5. Supplementary material

Crystallographic data (excluding structure factors) for the structures reported in this paper (Tables 8–10) have been deposited with the Cambridge Crystallographic Data Centre and allocated the deposition numbers CCDC-149809 (**2**), CCDC-149810 (**5**), CCDC-149811 (**7**), CCDC-149814 (**8**), CCDC-149815 (**9**), CCDC-149812 (**10**), CCDC-149816 (**13**), CCDC-149813 (**14·0.5Et_2O**), CCDC-149817 (**16**), CCDC-154353 [**(*R*,*R*)-3**], and CCDC-154354 [**(*S*,*S*)-3**]. Copies of this information may be obtained free of charge

Table 8
Selected crystallographic data for complexes **2**, **5**, **7**, and **8**

	2	**5**	**7**	**8**
Formula	$C_{25}H_{48}Cl_2N_4P_2Pt$	$C_{26}H_{51}ClN_4P_2Pt$	$C_{34}H_{39}ClP_2Pt$	$C_{30}H_{59}ClN_4P_2Pt$
M_r	732.6	712.2	740.1	768.3
Crystal size (mm)	$0.40 \times 0.28 \times 0.28$	$0.55 \times 0.10 \times 0.10$	$0.33 \times 0.28 \times 0.10$	$0.49 \times 0.45 \times 0.28$
Crystal system	tetragonal	monoclinic	monoclinic	monoclinic
Space group	$I\bar{4}2d$ (No. 122)	$P2_1/c$ (No. 14)	$P2_1/n$ (No. 14)	$P2_1/c$ (No. 14)
a (Å)	21.171(1)	11.699(3)	10.5420(5)	9.8120(9)
b (Å)	21.171(1)	17.234(2)	15.043(2)	18.3970(8)
c (Å)	13.5018(8)	14.829(1)	20.005(1)	18.794(4)
β (°)	90	90.66(5)	96.499(4)	93.44(1)
V (Å^3)	6052(1)	2990(1)	3152.0(4)	3386(1)
Z	8	4	4	4
d_{calc} (g cm^{-3})	1.608	1.582	1.560	1.507
μ(Mo–K_α) (mm^{-1})	4.940	4.911	4.659	4.342
T_{min}	0.2426	0.2918	0.3085	0.0880
T_{max}	0.3384	0.6042	0.6530	0.2750
θ range (°)	$2.63 \le \theta \le 25.97$	$2.10 \le \theta \le 24.00$	$2.05 \le \theta \le 26.97$	$2.54 \le \theta \le 25.08$
$h\ k\ l$ range	−26 26, 0 26, 0 16	0 13, 0 19, −16 16	−13 13, 0 19, 0 25	−11 11, 0 21, −22 0
Reflections collected	6249	4939	7053	6195
Unique reflections (R_{int})	2975 (0.0516)	4689 (0.0974)	6861 (0.0293)	6003 (0.0208)
Intensities $I > 2\sigma(I)$	2574	2895	4180	4523
Parameter/F_o ratio	155/2975	308/4689	346/6861	346/6003
wR_2 of F^2 (all data)	0.0679	0.2044	0.0716	0.0728
R_1 of F [$I > 2\sigma(I)$]	0.0300	0.0825	0.0371	0.0341
Goodness of fit on F^2	1.022	1.123	1.011	1.023

Table 9
Selected crystallographic data for complexes **9**, **10**, **13**, and **14·0.5 Et_2O**

	9	**10**	13	**14·0.5 Et_2O**
Formula	$C_{34}H_{39}ClO_4P_2Pt$	$C_{35}H_{70}N_4P_2Pt$	$C_{35}H_{39}F_3O_3P_2PtS$	$C_{63}H_{67}ClF_3O_{3.5}P_4Pt_2S$
M_r	804.1	804.0	853.7	1518.7
Crystal size (mm)	$0.48\times0.28\times0.15$	$0.20\times0.18\times0.15$	$0.35\times0.13\times0.10$	$0.33\times0.20\times0.03$
Crystal system	monoclinic	orthorhombic	monoclinic	triclinic
Space group	$P2_1/c$ (No. 14)	*Pbcn* (No. 60)	$P2_1/c$ (No. 14)	$P\bar{1}$ (No. 2)
a (Å)	10.136(2)	10.0576(4)	10.288(2)	9.264(2)
b (Å)	15.011(1)	17.515(3)	16.208(1)	16.299(5)
c (Å)	22.596(2)	21.271(1)	21.401(1)	20.833(4)
α (°)	90	90	90	77.46(2)
β (°)	90.40(1)	90	99.50(1)	81.95(1)
γ (°)	90	90	90	89.99(1)
V (Å^3)	3438(1)	3747(1)	3520(1)	3038(1)
Z	4	4	4	2
d_{calc} (g cm^{-3})	1.554	1.425	1.611	1.660
μ(Mo–K$_\alpha$) (mm^{-1})	4.287	3.858	4.186	4.838
T_{min}	0.2328	0.5125	0.3221	0.2261
T_{max}	0.5657	0.5953	0.6796	0.6996
θ range (°)	$2.58\le\theta\le26.97$	$2.52\le\theta\le29.96$	$2.51\le\theta\le25.07$	$2.50\le\theta\le24.97$
$h\ k\ l$ range	0 12, 0 19, −28 28	−1 14, −1 24, −1 29	−12 12, 0 19, 0 25	0 11, −19 19, −24 24
Reflections collected	7885	6672	6427	11364
Unique reflections (R_{int})	7456 (0.0344)	5448 (0.0313)	6249 (0.0468)	10 643 (0.0531)
Intensities $I>2\sigma(I)$	5139	2617	4133	6071
Parameter/F_o ratio	382/7465	203/5448	409/6249	642/10 643
wR_2 of F^2 (all data)	0.0725	0.0792	0.0851	0.1397
R_1 of F [$I>2\sigma(I)$]	0.0408	0.0445	0.0483	0.0622
Goodness of fit on F^2	1.028	1.023	1.021	1.012

Table 10
Selected crystallographic data for complexes **16, (*R*,*R*)-3**, and (***S*,*S*)-3**

	16	(***R*,*R*)-3**	(***S*,*S*)-3**
Formula	$C_{29}H_{28}Cl_4P_2PtSn$	$C_{29}H_{28}Cl_2O_4P_2Pt$	$C_{29}H_{28}Cl_2O_4P_2Pt$
M_r	894.0	768.4	768.4
Crystal size (mm)	$0.40\times0.20\times0.08$	$0.47\times0.36\times0.34$	$0.50\times0.50\times0.28$
Crystal system	monoclinic	monoclinic	monoclinic
Space group	$P2_1/c$ (No. 14)	$P2_1$ (No. 4)	$P2_1$ (No. 4)
a (Å)	22.019(1)	10.8014(8)	10.8031(5)
b (Å)	14.794(1)	14.889(3)	14.890(1)
c (Å)	22.210(1)	18.831(1)	18.848(3)
β (°)	119.366(5)	103.312(6)	103.31(1)
V (Å^3)	6305(1)	2947.1(6)	2950.4(5)
Z	8	4	4
d_{calc} (g cm^{-3})	1.884	1.732	1.730
μ(Mo–K$_\alpha$) (mm^{-1})	5.683	5.084	5.078
T_{min}	0.2096	0.1985	0.1856
T_{max}	0.6592	0.2768	0.3305
θ range (°)	$2.10\le\theta\le25.18$	$2.22\le\theta\le28.17$	$2.59\le\theta\le27.97$
$h\ k\ l$ range	0 26, 0 17, −26 23	−14 0, 0 19, −25 25	−14 0, 0 19, −24 24
Reflections collected	11 628	15 778 [a]	15 496 [a]
Unique reflections (R_{int})	11 315 (0.0681)	14 447 (0.0394)	14 209 (0.0426)
Intensities $I>2\sigma(I)$	4905	10 103	9809
Parameter/F_o ratio	721/11 315	685/14 447	685/14 209
wR_2 of F^2 (all data)	0.1873	0.1154	0.1052
R_1 of F [$I>2\sigma(I)$]	0.0824	0.0520	0.0540
Goodness of fit on F^2	1.013	1.006	1.025
Absolute structure parameter x [57]		0.003(9)	0.014(10)

[a] Including Friedel pairs.

from The Director, CCDC, 12 Union Road, Cambridge CB2 1EZ, UK (Fax: +44-1223-336033; e-mail: deposit@ccdc.cam.ac.uk).

Acknowledgements

Financial support from the Deutsche Forschungsgemeinschaft (Bonn) and the Fonds der Chemischen Industrie (Frankfurt/Main) is gratefully acknowledged. We are also indebted to Degussa-Hüls AG (Hanau) for a generous gift of platinum salts. Gas chromatographic analyses were carried out at the Institut für Organische Chemie, Universität Regensburg. We gratefully acknowledge the help of Professor Dr B. König and Dr E. Eibler.

References

[1] L. Dahlenburg, R. Götz, J. Organomet. Chem. 619 (2001) 88.
[2] Review articles:(a) C. Botteghi, S. Paganelli, A. Schionato, M. Marchetti, Chirality 3 (1991) 355;
(b) F. Agbossou, J.-F. Carpentier, A. Mortreux, Chem. Rev. 95 (1995) 2485;
(c) C.D. Frohning, C.W. Kohlpaintner, in: B. Cornils, W.A. Herrmann (Eds.), Applied Homogeneous Catalysis with Organometallic Compounds, VCH, Weinheim, 1996, Chapter 2.1.1;
(d) F. Ungváry, Coord. Chem. Rev. 188 (1999) 263.
[3] (a) C.U. Pittman, Jr., Y. Kawabata, L.I. Flowers, J. Chem. Soc. Chem. Commun. (1982) 473;
(b) G. Consiglio, P. Pino, L.I. Flowers, C.U. Pittman, J. Chem. Soc. Chem. Commun. (1983) 612;
(c) G. Consiglio, S.C.A. Nefkens, A. Borer, Organometallics 10 (1991) 2046.
[4] (a) G. Parinello, J.K. Stille, J. Am. Chem. Soc. 109 (1987) 7122;
(b) J.K. Stille, H. Su, P. Brechot, G. Parinello, L.S. Hegedus, Organometallics 10 (1991) 1183.
[5] (a) S. Cserépi-Szücs, J. Bakos, Chem. Commun. (1997) 635;
(b) S. Cserépi-Szücs, G. Huttner, L. Zsolnai, J. Bakos, J. Organomet. Chem. 586 (1999) 70.
[6] (a) J.E. Babin, G.T. Whiteker (Union Carbide Chemicals and Plastics Technology Corp.), PCT Int. Appl. WO 9303839, 1993 [Chem. Abstr. 119 (1993) 159872];
(b) J.E. Babin, G.T. Whiteker (Union Carbide Chemicals and Plastics Technology Corp.), US 5360938, 1994 [Chem. Abstr. 122 (1995) 186609].
[7] (a) G.J.H. Buisman, E.J. Vos, P.C.J. Kamer, P.W.N.M. van Leeuwen, J. Chem. Soc. Dalton Trans. (1995) 409;
(b) G.J.H. Buisman, L.A. van der Veen, A. Klootwjik, W.G.J. de Lange, P.C.J. Kamer, P.W.N.M. van Leeuwen, D. Vogt, Organometallics 16 (1997) 2929;
(c) S. Deerenberg, P.C.J. Kamer, P.W.N.M. van Leeuwen, Organometallics 19 (2000) 2065.
[8] (a) N. Sakai, S. Mano, K. Nozaki, H. Takaya, J. Am. Chem. Soc. 115 (1993) 7033;
(b) T. Horiuchi, T. Ohta, E. Shirakawa, K. Nozaki, H. Takaya, J. Org. Chem. 62 (1997) 4285;
(c) K. Nozaki, N. Sakai, T. Nanno, T. Higashijima, S. Mano, T. Horiuchi, H. Takaya, J. Am. Chem. Soc. 119 (1997) 4413;
(d) K. Nozaki, Y. Itoi, F. Shibahara, E. Shirakawa, T. Ohta, H. Takaya, T. Hiyama, J. Am. Chem. Soc. 120 (1998) 4051;
(e) K. Nozaki, H. Takaya, T. Hiyama, Top. Catal. 4 (1998) 175;
(f) K. Nozaki, F. Shibahara, Y. Itoi, E. Shirakawa, T. Ohta, H. Takaya, T. Hiyama, Bull. Chem. Soc. Jpn. 72 (1999) 1911.
[9] D. Gleich, R. Schmid, W.A. Herrmann, Organometallics 17 (1998) 4828.
[10] (a) G. Francio, W. Leitner, Chem. Commun. (1999) 1663;
(b) W. Leitner, S. Kainz, D. Koch, G. Francio (Studiengesellschaft Kohle m.b.H., Germany), Ger. Offen. DE 19853748, 2000 [Chem. Abstr. 133 (2000) 4527].
[11] R. Kadyrov, D. Heller, R. Selke, Tetrahedron Asymmetry 9 (1998) 329.
[12] (a) D.L. Allen, V.C. Gibson, M.L.H. Green, J.F. Skinner, J. Bashkin, P.D. Grebenik, J. Chem. Soc. Chem. Commun. (1983) 895;
(b) M.L.H. Green (British Petroleum Co. PLC), Eur. Pat. Appl. EP 117156, 1984 [Chem. Abstr. 102 (1985) 6809].
[13] (a) C. Eckert, L. Dahlenburg, A. Wolski, Z. Naturforsch. B: Chem. Sci. 50b (1995) 1004;
(b) L. Dahlenburg, V. Kurth, Eur. J. Inorg. Chem. (1998) 597;
(c) L. Dahlenburg, A. Kaunert, Acta Crystallogr, Sect. C: Cryst. Struct. Commun. C 54 (1998) 1016;
(d) L. Dahlenburg, C. Becker, J. Höck, S. Mertel, J. Organomet. Chem. 564 (1998) 155;
(e) L. Dahlenburg, A. Kaunert, Eur. J. Inorg. Chem. (1998) 885;
(f) L. Dahlenburg, C. Eckert, J. Organomet. Chem. 564 (1998) 227;
(g) L. Dahlenburg, Ger. Offen. DE 19732805, 1999 [Chem. Abstr. 130 (1999) 168481];
(h) L. Dahlenburg, V. Kurth, J. Organomet. Chem. 585 (1999) 315.
[14] H. Brunner, S. Stefaniak, M. Zabel, Synthesis (1999) 1776.
[15] Application as ligands in conventional hydroformylation:
(a) S.-H. Kyung, Han'guk Nonghwa Hakhoechi 40 (1997) 588 [Chem. Abstr. 128 (1998) 154205];
(b) H. Urata, Y. Wada (Mitsubishi Chemical Industries Ltd., Japan), Jpn. Kokai Tokkyo Koho JP 09268152, 1997 [Chem. Abstr. 127 (1997) 307164];
(c) H. Urata, Y. Wada (Mitsubishi Chemical Industries Ltd., Japan), PCT Int. Appl. WO 9843935, 1998 [Chem. Abstr. 129 (1998) 289879];
(d) H. Maas, R. Paciello, M. Röper, J. Fischer, W. Siegel (BASF A.-G., Germany), PCT Int. Appl. WO 9946044, 1999 [Chem. Abstr. 131 (1999) 230267];
(e) D. Selent, K.-D. Wiese, D. Röttger, A. Börner, Angew. Chem. 112 (2000) 1694; Angew. Chem. Int. Ed. 39 (2000) 1639.
[16] (a) T.V. RajanBabu, T.A. Ayers, Tetrahedron Lett. 35 (1994) 4295;
(b) X. Xu, H. Zhou, J. Chen, H. Fu, Fenzi Cuihua 11 (1997) 374 [Chem. Abstr. 128 (1998) 4864];
(c) R. Ewalds, E.B. Eggeling, A.C. Hewat, P.C.J. Kamer, P.W.N.M. van Leeuwen, D. Vogt, Chem. Eur. J. 6 (2000) 1496.
[17] G.K. Anderson, H.C. Clark, J.A. Davies, Organometallics 1 (1982) 64.
[18] (a) R. Bardi, A.M. Piazzesi, G. Cavinato, P. Cavoli, L. Toniolo, J. Organomet. Chem. 224 (1982) 407;
(b) R. Bardi, A.M. Piazzesi, A. del Pra, G. Cavinato, L. Toniolo, J. Organomet. Chem. 234 (1982) 107;
(c) G. Cavinato, L. Toniolo, J. Organomet. Chem. 241 (1983) 275;
(d) A. Scrivanti, A. Berton, L. Toniolo, C. Botteghi, J. Organomet. Chem. 314 (1986) 369;
(e) H.J. Ruegg, P.S. Pregosin, A. Scrivanti, L. Toniolo, C. Botteghi, J. Organomet. Chem. 316 (1986) 233;
(f) A. Scrivanti, C. Botteghi, L. Toniolo, A. Berton, J. Organomet. Chem. 344 (1988) 261.
[19] M. Gómez, G. Muller, D. Sainz, J. Sales, X. Solans, Organometallics 10 (1991) 4036.

[20] (a) I. Tóth, T. Kégl, C.J. Elsevier, L. Kollár, Inorg. Chem. 33 (1994) 5798;
(b) T. Kégl, L. Kollár, L. Radics, Inorg. Chim. Acta 265 (1997) 249;
(c) E. Farkas, L. Kollár, M. Moret, A. Sironi, Organometallics 15 (1996) 1345;
(d) T. Kégl, L. Kollár, J. Mol. Catal. A Chem. 122 (1997) 95.
[21] J.J. Mrowca (du Ponts de Nemours, E.I. and Co.), US 3876672, 1975 [Chem. Abstr. 84 (1976) 30432].
[22] S.C. Tang, L. Kim, J. Mol. Catal. 14 (1982) 231.
[23] (a) P.W.N.M. van Leeuwen, C.F. Roobeek (Shell Research B.V.), Eur. Pat. Appl. EP 82576, 1983 [Chem. Abstr. 99 (1983) 121813];
(b) P.W.N.M. van Leeuwen, C.F. Roobeek, R.L. Wife, J.H.G. Frijns, J. Chem. Soc. Chem. Commun. (1986) 31;
(c) P.W.N.M. van Leeuwen, C.F. Roobeek, J.H.G. Frijns, A.G. Orpen, Organometallics 9 (1990) 1211;
(d) P.W.N.M. van Leeuwen, C.F. Roobeek, New J. Chem. 14 (1990) 487.
[24] E. Paumard, A. Mortreux, F. Petit, J. Chem. Soc. Chem. Commun. (1989) 1380.
[25] (a) C. Botteghi, S. Paganelli, U. Matteoli, A. Scrivanti, R. Ciorciaro, L.M. Venanzi, Helv. Chim. Acta 73 (1990) 284;
(b) C. Botteghi, S. Paganelli, A. Perosa, R. Lazzaroni, G. Uccello–Barretta, J. Organomet. Chem. 447 (1993) 153.
[26] R.L. Brainard, W.R. Nutt, T.R. Lee, G.M. Whitesides, Organometallics 7 (1988) 2379.
[27] A. Appelt, V. Ariaratnam, A.C. Willis, S.B. Wild, Tetrahedron Asymmetry 1 (1990) 9.
[28] (a) L. Mole, J.L. Spencer, N. Carr, A.G. Orpen, Organometallics 10 (1991) 49;
(b) N. Carr, L. Mole, A.G. Orpen, J.L. Spencer, J. Chem. Soc. Dalton Trans. (1992) 2653.
[29] (a) P.J. Stang, Y.-H. Huang, J. Organomet. Chem. 431 (1992) 247;
(b) P.J. Stang, Z. Zhong, A.M. Arif, Organometallics 11 (1992) 1017.
[30] G.P.C.M. Dekker, A. Buijs, C.J. Elsevier, K. Vrieze, P.W.N.M. van Leeuwen, W.J.J. Smeets, A.L. Spek, Y.F. Wang, C.H. Stam, Organometallics 11 (1992) 1937.
[31] B.L. Bennett, J. Birnbaum, D. Roddick, Polyhedron 14 (1995) 187.
[32] (a) G.S. Hill, L.M. Rendina, R.J. Puddephatt, J. Chem. Soc. Dalton Trans. (1996) 1809;
(b) G.S. Hill, G.P.A. Yap, R.J. Puddephatt, Organometallics 18 (1999) 1408.
[33] (a) J. Chatt, L.M. Vallarino, L.M. Venanzi, J. Chem. Soc. (1957) 2496;
(b) H.C. Clark, L.E. Manzer, J. Organomet. Chem. 59 (1973) 411;
(c) J.X. McDermott, J.F. White, G.M. Whitesides, J. Am. Chem. Soc. 98 (1976) 6521;
(d) R.L. Brainard, T.M. Miller, G.M. Whitesides, Organometallics 5 (1986) 1481.
[34] (a) D.A. Redfield, J.H. Nelson, L.W. Cary, Inorg. Nucl. Chem. Lett. 10 (1974) 727;
(b) A.W. Verstuyft, J.H. Nelson, L.W. Cary, Inorg. Chem. 15 (1976) 732.
[35] P.S. Pregosin, R. Kunz, Helv. Chim. Acta 58 (1975) 423.
[36] G.K. Anderson, in: E.W. Abel, F.G.A. Stone, G. Wilkinson (Eds.), Comprehensive Organometallic Chemistry II, Vol. 9 (R.J. Puddephatt, Ed.), Pergamon Press, Oxford, 1995, Chapter 8.
[37] (a) F. Bachechi, Acta Crystallogr. Sect. C Cryst. Struct. Commun. C 49 (1993) 460;
(b) F. Bachechi, P. Mura, L. Zambonelli, Acta Crystallogr. Sect. C Cryst. Struct. Commun., C 49 (1993) 2072;
(c) A. Albinati, S. Chaloupka, J. Eckert, L.M. Venanzi, M.K. Wolfer, Inorg. Chim. Acta 259 (1997) 305;
(d) A. Albinati, G. Bracher, D. Carmona, J.H.P. Jans, W.T. Klooster, T.F. Koetzle, A. Macchioni, J.S. Ricci, R. Thouvenot, L.M. Venanzi, Inorg. Chim. Acta 265 (1997) 255 and references cited therein.
[38] M. Gerisch, F.W. Heinemann, C. Bruhn, J. Scholz, D. Steinborn, Organometallics 18 (1999) 564 and references cited therein.
[39] S.A. Litster, L. Mole, A.D. Redhouse, J.L. Spencer, Acta Crystallogr. Sect. C Cryst. Struct. Commun. C 48 (1992) 913.
[40] P. Meessen, D. Vogt, W. Keim, J. Organomet. Chem. 551 (1998) 165.
[41] (a) L. Kollár, J. Bakos, I. Tóth, B. Heil, J. Organomet. Chem. 350 (1988) 277;
(b) L. Kollar, P. Sándor, G. Szalontai, J. Mol. Catal. 67 (1991) 191;
(c) L. Kollár, T. Kégl, J. Bakos, J. Organomet. Chem. 453 (1993) 155;
(d) I. Tóth, I. Guo, B.E. Hanson, Organometallics 12 (1993) 848;
(e) I. Tóth, C.J. Elsevier, J.G. de Vries, J. Bakos, W.J.J. Smeets, A.L. Spek, J. Organomet. Chem. 540 (1997) 15.
[42] (a) A. Scrivanti, S. Zeggio, V. Beghetto, U. Matteoli, J. Mol. Catal. A Chem. 101 (1995) 217;
(b) A. Scrivanti, V. Beghetto, A. Bastianini, U. Matteoli, G. Menchi, Organometallics 15 (1996) 4687.
[43] L. Kollár, G. Consiglio, P. Pino, J. Organomet. Chem. 300 (1987) 305.
[44] I. Schwager, J.F. Knifton, J. Catal. 45 (1976) 256.
[45] C.Y. Hsu, M. Orchin, J. Am. Chem. Soc. 97 (1975) 3553.
[46] F. Ozawa, T. Hikida, K. Haebe, T. Mori, Organometallics 17 (1998) 1018.
[47] E.V. van den Berghe, G.P. van der Kelen, J. Organomet. Chem. 6 (1966) 515.
[48] H.C. Clark, G. Ferguson, M.J. Hampden-Smith, H. Rüegger, B.L. Ruhl, Can. J. Chem. 66 (1988) 3120.
[49] G. Cavinato, G. de Munno, M. Lami, M. Marchionna, L. Toniolo, D. Viterbo, J. Organomet. Chem. 466 (1994) 277.
[50] A. Albinati, N. Naegeli, K.H.A. Ostoja Starzewski, P.S. Pregosin, H. Rüegger, Inorg. Chim. Acta 76 (1983) L231–L232.
[51] R. van Asselt, E. Rijnberg, C.J. Elsevier, Organometallics 13 (1994) 706.
[52] A.C.T. North, D.C. Phillips, F.S. Mathews, Acta Crystallogr. A 24 (1968) 351.
[53] L.J. Farrugia, WinGX (Version 1.63.01) — An Integrated System of Windows Programs for the Solution, Refinement, and Analysis of Single Crystal X-ray Diffraction Data, University of Glasgow, 1999; J. Appl. Crystallogr. 32 (1999) 837.
[54] A. Altomare, G. Cascarano, C. Giacovazzo, A. Guagliardi, A.G.G. Moliterni, M.C. Burla, G. Polidori, M. Camalli, R. Spagna, SIR-97 — A Package for Crystal Structure Solution by Direct Methods and Refinement, Bari, Rome, 1997.
[55] G.M. Sheldrick, SHELXL-97 — A Program for the Refinement of Crystal Structures from Diffraction Data (Release 97-2), Universität Göttingen, 1997.
[56] L.J. Farrugia, ORTEP-3 for Windows (Version 1.062), University of Glasgow, 1997/2000; J. Appl. Crystallogr. 30 (1997) 565.
[57] H.D. Flack, Acta Crystallogr. A 39 (1983) 876.